DEPARTMENT OF TRANSPORTATION

Development of a Queue Warning System Utilizing ATM Infrastructure System Development and Field Testing

John Hourdos, Principal Investigator
Minnesota Traffic Observatory
Deparment of Civil, Environmental, and Geo-Engineering
University of Minnesota

June 2017

Research Project
Final Report 2017-20

LRRB
LOCAL ROAD RESEARCH BOARD

To request this document in an alternative format, such as braille or large print, call 651-366-4718 or 1-800-657-3774 (Greater Minnesota) or email your request to ADArequest.dot@state.mn.us. Please request at least one week in advance.

Technical Report Documentation Page

1. Report No.	2.	3. Recipients Accession No.
MN/RC 2017-20		

4. Title and Subtitle	5. Report Date
Development of a Queue Warning System Utilizing ATM Infrastructure System Development and Field-Testing.	June 13, 2017
	6.

7. Author(s)	8. Performing Organization Report No.
John Hourdos, Zhejun Liu, Peter Dirks, Henry X. Liu, Shihong Huang, Weili Sun, Lin Xiao	

9. Performing Organization Name and Address	10. Project/Task/Work Unit No.
Civil, Environmental, and Geo-Engineering University of Minnesota – Twin Cities 500 Pillsbury Dr SE, Minneapolis MN, 55455	2015008
	11. Contract (C) or Grant (G) No. (C) 99008 (wo) 154

12. Sponsoring Organization Name and Address	13. Type of Report and Period Covered
Minnesota Local Road Research Board Minnesota Department of Transportation Research Services & Library 395 John Ireland Boulevard, MS 330 St. Paul, Minnesota 55155-1899	Final Report
	14. Sponsoring Agency Code

15. Supplementary Notes

http:// mndot.gov/research/reports/2017/201720.pdf

16. Abstract (Limit: 250 words)

MnDOT has already deployed an extensive infrastructure for Active Traffic Management (ATM) on I-35W and I-94 with plans to expand on other segments of the Twin Cities freeway network. The ATM system includes intelligent lane control signals (ILCS) spaced every half mile over every lane to warn motorists of incidents or hazards on the roadway ahead. This project developed two separate systems that can identify lane-specific shockwave or queuing conditions on the freeway and use existing ILCS to warn motorists upstream for rear-end collision prevention. The two systems were field tested at two locations in the ATM equipped network that have a high frequency of rear-end collisions. These locations experience significantly different traffic-flow conditions, allowing for the development and testing of two different approaches to the same problem. The I-94 westbound segment in downtown Minneapolis is known for its high crash rate due to rapidly evolving shockwaves while the I-35W southbound segment north of the TH-62 interchange experiences longstanding queues extending into the freeway mainline. The Minnesota Traffic Observatory developed the I-94 Queue Warning system while the University of Michigan, under contract, developed the I-35W system. Prior to the I-94 installation, based on data collected in 2013, there were 11.9 crashes per VMT and 111.8 near crashes per VMT. In the first three months of the system's deployment, event frequency reduced to 9.34 crashes per million vehicle miles of travel (MVMT) and 51.8 near crashes per MVMT, a 22% decrease in crashes and a 54% decrease in near crashes. The I-35W system did not undergo a similarly thorough evaluation, but for most of the lane segments involved, it showed that queue warning messages help reduce the speed variance near the queue locations and the speed difference between upstream and downstream locations. This also implicated a satisfactory level of compliance rate from travelers.

17. Document Analysis/Descriptors	18. Availability Statement
queuing, warning signs, highway safety, shock waves, physical distribution, highway traffic control	No restrictions. Document available from: National Technical Information Services, Alexandria, Virginia 22312

19. Security Class (this report)	20. Security Class (this page)	21. No. of Pages	22. Price
Unclassified	Unclassified	86	

Development of a Queue Warning System Utilizing ATM Infrastructure System Development and Field Testing.

FINAL REPORT

Prepared by:

John Hourdos
Zhejun Liu
Peter Dirks
Minnesota Traffic Observatory
Department of Civil, Environmental, and Geo-Engineering
University of Minnesota

Henry X. Liu
Shihong Huang
Weili Sun
Lin Xiao
Department of Civil and Environmental Engineering
University of Michigan

June 2017

Published by:

Minnesota Department of Transportation
Research Services & Library
395 John Ireland Boulevard, MS 330
St. Paul, Minnesota 55155-1899

ACKNOWLEDGMENTS

This work was supported by the Minnesota Department of Transportation (MnDOT). The authors would like to thank Brian Kary, Jesse Larson and Douglas Lau of MnDOT for their assistance in this project. The authors would also like to thank Gordon Parikh and Derek Lehrke at the Minnesota Traffic Observatory University of Minnesota for helping to record video data and maintaining the data collection infrastructure. The research team would also like to acknowledge the support this project has received from the Roadway Safety Institute, the University Transportation Center for USDOT Region 5 under the Moving Ahead for Progress in the 21st Century Act (MAP-21) federal transportation bill passed in 2012.

TABLE OF CONTENTS

LIST OF FIGURES

LIST OF TABLES

EXECUTIVE SUMMARY

In 2014, the Minnesota Department of Public Safety (DPS) reported 15,648 crashes occurred on Minnesota freeways. These crashes accounted for the death of 38 people and the injury of 5,031 people (3). Rear-end crashes are a typical type of crash on freeways. Although, rear-end crashes can happen any time there is a disturbance, research has shown (4) that there are traffic conditions that are associated with collisions, specifically rear-end collisions. Prior studies have shown that such crash prone traffic Conditions (CPCs) can be detected over other traffic conditions encountered on freeway traffic.

The research described in this report aimed to develop and field test two queue warning systems using different philosophies in regard to rear-end collision safety. The first system's philosophy, follows the premise that freeway rear-end collisions tend to occur in extended stop-and-go traffic or at end-of-queue locations (29). Such unconditional queue warning systems usually provide warning messages in an unselective manner, i.e., react to all the queues based on the assumption that all propagating queues are dangerous and drivers should be warned. Conditions on I-35W southbound in Minneapolis, MN, support this hypothesis, and it is there where the first system prototype was developed and deployed. This system was developed by a research team lead by Dr. Henry Liu at the University of Michigan. The second queue warning system is based on the hypothesis that not all congestion events are dangerous but there are certain traffic conditions that are crash prone regardless of whether they result in standing queues or not. Such CPCs can be isolated, fast moving shockwaves, involving only a small number of vehicles in the deceleration-stop-acceleration cycle. For such conditions, a much more dense detection infrastructure is needed. One location where such conditions have been identified and result in more than 100 crashes per year is the westbound section of I-94 in downtown Minneapolis. In this location, the Minnesota Traffic Observatory has had a permanent Field Lab since 2002. Based on the framework proposed by Dr. Hourdos (4), this effort approaches the topic from the quantification of traffic flow to the multi-layer system design along with different approaches including traffic assessment modeling and the development of control algorithms. This approach utilizes individual vehicle measurements including individual vehicle speeds and time headways, as the major type of data for the system operation. The prototype of a CPC detection-based queue warning system was developed by a research team lead by Dr. John Hourdos at the University of Minnesota.

I-94 WB Queue Warning System Description and Results

The I-94 CPC Queue Warning system follows a three-layer design. The crash probability layer collects real-time individual vehicle measurements and processes them to remove noise. The filtered data then pass to the crash-probability model to assess the likelihood of a crash. This crash likelihood along with additional traffic information, such as speeds and headways, are passed to the second layer, the algorithm layer. In this layer, the algorithm decides if a warning message should be generated by comparing the crash probability with preset thresholds and real-time traffic conditions. A decision of whether to raise or drop the alarm is being generated and passed to the third layer, system control, in which requirements from policy makers are applied to modify the result before delivering it to the message sign in the field. Specifically, as part of the terms for the deployment of the system, two overrides were included and the preexisting MnDOT signs' refresh rate was kept. Two sets of Intelligent

Lane Control Signs (ILCSs) are used to communicate the warnings to the drivers. The overrides are intended to limit possible overexposure of drivers to the warning by what was, at the time of implementation, an unproven system and consist of a time override and a congestion override. The time override prevents the sign from being turned on, regardless of the alarm status before noon or after 8 p.m. The congestion override also prevents the sign from being turned on when five consecutive 30-second average speed measurements at the loop detector near the farthest upstream sign are below 25 mph. This override is intended to reduce driver overexposure to the warning by not displaying a warning when drivers are already travelling slowly. The rate at which the sign is updated is a result of the sign being part of the MnDOT Twin Cities metro-wide network. Initial activation can vary from a few seconds to one minute, depending on the synchronization between the independent queue warning system and the traffic operations system that controls the signs. This delay amplifies short gaps in the alarm activation.

To obtain the ground truth on which the I-94 system was evaluated, event observations were collected during a three-month evaluation period (from June 2016 to August 2016). This involved manual reduction of video from multiple cameras recording crashes and near-crashes, as well as the exact times the sign changed states. Data from 55 weekdays with sufficient video footage in this period were used to establish ground truth. Some weekdays were excluded due to corrupted video files or equipment maintenance. Based on the ground truth established, detection rates under different system conditions were calculated. To assess the performance of the system, the detection rate of all conflict events between 3rd Ave and Chicago Ave during the three-month evaluation period was calculated separately for the control algorithm and for the system as a whole. The detection rate was calculated for just the crashes, near crashes, and both events combined. To find the actual number of conflict events, all the events observed during the evaluation period were tabulated and sorted based on whether the drivers involved were warned or not warned about crash-prone conditions before the event, and if not, separated by the reason for such failure.

Detecting Component	**Event Type**		
	Crashes	**Near Crashes**	**Both**
	[%]	**[%]**	**[%]**
Algorithm (9 a.m. to 8 p.m.)	76.3	79.3	78.6
Whole System (9 a.m. to 8 p.m.)	39.5	51.9	49.0
Algorithm (noon to 8 p.m.)	73.5	74.6	74.3
Whole System (noon to 8 p.m.)	44.1	63.6	59.2

The control algorithm is far more successful at raising the alarm for events than the system as a whole. The noon to 8 p.m. group illustrated the effect of the congestion override, a subject that was raised as a concern to MnDOT. A 2013 study recorded crashes that occurred between MN 65 and Portland Ave. These results are compared to the 2016 events that occurred in the same region. Based on the comparison of the two periods, there was a 22% decrease in crashes and a 54% decrease in near crashes in that zone following the implementation of the I-94 CPC Queue Warning system.

Observation Zone	MN 65 to Portland Ave		% Reduction
Observation Year	**2013**	**2016**	**2013 vs 2016**
Crashes	11.9	9.34	-22%
Near Crashes	111.8	51.8	-54%

MnDOT is considering the results from the I-94 CPC Queue Warning system promising and is considering an extended evaluation to look at the long-term effects of the system on crash rates.

I-35W SB Queue Warning System Description and Results

The I-35W SB Queue Warning system developed by Dr. Liu utilizes data collected from five sets of Systematic Monitoring of Arterial Road Traffic Signal (SMART-Signal) systems installed on MnDOT detector cabinets. The SMART-Signal system collects and archives high-resolution vehicle-detector actuation events. Each event contains the timestamp and occupancy time of one vehicle as well as the ID of the corresponding detector. The difference between the arrival times of consecutive vehicles gives the headway for these two vehicles and taking the occupancy time out of the headway gives the gap between these two vehicles. Based on the real-time data collected from detectors, the Michigan Queue Warning Algorithm (MQWA) can "see" a queue when it travels to the position of a detector. Although traffic states from detectors upstream and downstream of the queue occurrence position give some implication of the jam, it is risky to predict the occurrence of queue before it reaches a detector because such prediction easily generates false alarms. Therefore, instead of capturing the exact occurrence time and location of every stopped queue, the MQWA works to monitor the queue once it is seen by detectors. For those queues starting from in-between positions and propagating to detectors, lags in response arise but the MQWA provides a more robust solution than capturing the exact occurrence time and location of every stopped queue. For queues not propagating to detectors, the MQWA omits them because of their limited influence in space and time. Instances of the MQWA can run locally in any freeway segment between two detectors, estimating the length and duration of a queue once it is detected by the downstream detector. Moreover, considering the difference of traffic states across lanes (e.g., lanes to different directions of a diverge junction), one instance of the MQWA can run for each lane. The MQWA has limited capability of prediction about the time when a queue will be formed or cleared at any position in this segment, or the queue length in this segment at any time in the near future.

The MQWA was implemented on a 2,218-foot-long I-35W SB segment between 50th and 60th Streets in South Minneapolis. The system was tested in the field for three weeks, showing the queue warning message "SLOW TRAFFIC AHEAD" to travelers when a queue was estimated at downstream locations. Before that, the system had also been running for three weeks without actually showing messages. The high-resolution data from loop detectors, the queue warning system log files archiving the start time, duration and location of triggered messages (including those not shown on the ILCS before field test), and videos from MnDOT cameras were used to evaluate the queue warning system. Based on the before and after data collected, the mean value and standard deviation of speed was calculated for each detector and for each message, and then a hypothesis testing was carried out to see whether there was

a significant change before and after the deployment of the system. Based on this evaluation methodology the following conclusions were drawn:

1. In general, travelers on I-35W did respond to the queue-warning message "SLOW TRAFFIC AHEAD" and the traffic conditions with and without messages showed statistically significant differences.
2. The MQWA was able to smooth traffic by reducing the speed variance at downstream locations and speed difference between upstream and downstream locations, and therefore reduced the risk of rear-end crash and potentially improved mobility.
3. It took travelers some time from seeing the messages to taking actions such as slowing down their vehicles. Consequently, queue warning messages had little to do with the traffic conditions near the ILCS gantry (50th Street) but had an evident impact on the traffic at downstream locations (Diamond Lake Road).
4. The standard deviation of speed at the bifurcation location was increased when the traffic condition farther downstream locations on TH-62 was continuously congested. This might be because the traffic state in this case was more influenced by the downstream congestion rather than the upstream arrival, which made the queue warning message not very effective.
5. There was no significant difference between the effect of warning message in the morning peak and that in the evening peak.

At the time of the writing of this report, both queue warning systems were still in operation. Starting in April 2018, the I-94 WB segment where the CPC Queue Warning system was operating will be under construction for three years. MnDOT has expressed the desire to implement two instances of the CPC Queue Warning upstream of the construction zone to alleviate concerns of rear-end collisions generated from congestion shockwaves due to capacity reduction in the work zone.

CHAPTER 1: INTRODUCTION

As the world's population continues to rise, roadways are utilized to and beyond the limits for which they were designed. This destabilizes traffic on freeways and produces dangerous driving conditions. In 2014, US officials reported the occurrence of 6.1 million crashes. These crashes injured 2.3 million people and killed 32,675 people (1). According to the Minnesota Department of Transportation (MnDOT), the average cost of a single crash is $7,600 when it involves only property damage, $83,000 to $570,000 when it involves injury, and as high as $10.6 million when the crash is fatal (2). In 2014, the Minnesota Department of Public Safety (DPS) reported 15,648 crashes occurred on Minnesota freeways. These crashes accounted for the death of 38 people and the injury of 5,031 people (3). Rear-end crashes are a typical type of crash that occurs on freeways. Although, rear-end crashes can happen any time there is a disturbance, research has shown (4) that there are traffic conditions that are associated with collisions, specifically rear-end collisions. Prior studies have shown that such crash prone traffic conditions (CPCs) can be detected and differentiated from other freeway traffic conditions encountered.

Discerning what factors influence crash rates and the way in which they do so has been the aim of many research projects. Qiu and Nixon (5) reviewed the effects of weather on the likelihood of a crash. Kopelias et al. (6) studied how the combined effects of geometric, operational, and weather factors influence crash frequencies. Traffic on urban freeways, however, tends to react differently to those factors. Golob and Recker (7) found that although collision with objects and the crashes of multiple vehicles are more frequent on wet roads, rear-end crashes are more likely to occur on dry roads with good visibility. They proposed that these rear-end crashes are highly correlated to large differences in individual speed like those seen in "stop-and-go" traffic. Such traffic conditions are often referred to as traffic shockwaves or traffic oscillations. Zheng et al. (8) studied the effects of traffic oscillations on freeway crashes and found that traffic oscillations and congestion are highly correlated to freeway crashes.

Various crash-prediction models (9-14) have been developed using the aforementioned factors. In such models, crash probability is used as a measure of the likelihood of a crash. Significant association has been shown between crash probability and traffic conditions. Hourdos et al. (4) utilized crash probability to detect CPCs on a freeway in Minneapolis, MN. While different approaches to apply crash-prediction models in real-time environments have been proposed (14-16), implementation of such models into real-time systems is rare.

A common application for dynamic queue warning systems is in work zones where the reduced capacity of the roadway cannot accommodate normal traffic volumes. Two systems designed for this application employ several sensors along the road upstream of the construction zone to detect the location of the upstream end of the queue. The first queue-warning system (17) uses live remote traffic microwave sensor (RTMS) data from two sensors (one immediately upstream of the work area and one at the end of the work area) to extrapolate the location of the back of the queue. The location of the back of the queue is then displayed on a portable changeable message sign (PCMS) at the location of the upstream

sensor. The second queue-warning system (18) uses up to eight speed sensors spread out over seven miles to detect queues. The system warns drivers approaching the work zone of any queues present through several upstream PCMSs. The Texas Department of Transportation used the eight-sensor system in a 96-mile project and found it lowered crash rates by as much as 47% when compared to an estimate of what they would have been had the system not been deployed.

For metropolitan areas where congestion is commonplace, slightly different approaches are often employed. One system in Houston, TX, (19) uses machine vision detectors (MVDs) to measure the speeds of vehicles approaching the area in which congestion generally occurs. When the system detects three consecutive vehicles with speeds lower than 25 mph, lights flash above a warning sign. Pesti et al. report decreases of 2% to 6% in vehicle conflicts when this queue warning system is in place. Another queue warning system deployed on a congestion-prone freeway is in Eugene, OR (20). The system measures freeway occupancy using three side-fire, dual-beam traffic detectors. When the freeway vehicle occupancy exceeds thresholds established by the Oregon Department of Transportation (ODOT), warnings are displayed on the Portable Changeable Message Signs (PCMSs) until the occupancy no longer exceeds the threshold along with a minimum display time of 5 minutes. The system is reported to have decreased the crash rate by over 35%.

The United States Department of Transportation (USDOT) is currently developing a connected-vehicle traffic management system called Intelligent Network Flow Optimization (INFLO) that incorporates queue warning components but it has not been deployed to date (21). The system relies on vehicle-to-infrastructure communication to share traffic data for the purpose of warning drivers of queues, harmonizing speed limits, and coordinating cruise control speeds of platooning vehicles. This report presents the design, specification, implementation and evaluation of two infrastructure-based queue warning systems that are capable of detecting dangerous traffic conditions, i.e., crash-prone conditions, on freeways and delivering warning messages to drivers, in order to increase their alertness to these traffic conditions and ultimately reduce the crash frequency on urban freeways.

The two queue warning systems were developed and field-tested using different philosophies in regard to rear-end collision safety. The first system's philosophy, shared by most of the aforementioned systems, follows the premise that freeway rear-end collisions tend to occur in extended stop-and-go traffic or at end-of-queue locations (29). Such unconditional queue warning systems usually provide warning messages in an unselective manner, i.e., react to all the queues based on the assumption that all propagating queues are dangerous and drivers should be warned. Conditions on I35W southbound in Minneapolis, MN, support this hypothesis and it is there where the first system prototype was developed and deployed. This system was developed by a research team at the University of Michigan lead by Dr Henry Liu and is described in Chapter 3. The second queue warning system is based on the hypothesis that not all congestion events, forming queues are dangerous but there are certain traffic conditions that are Crash Prone regardless of whether they result in standing queues or not. Such CPCs can be isolated, fast-moving shockwaves involving only a small number of vehicles in the deceleration-stop-acceleration cycle. For such conditions, a much denser detection infrastructure is needed. One location where such conditions have been identified and result in more than 100 crashes per year is the

westbound section of I-94 in downtown Minneapolis, MN. In this location, the Minnesota Traffic Observatory has had a permanent Field Lab since 2002. Based on the framework proposed by Hourdos (*4*), this effort approaches the topic from the quantification of traffic flow to the multi-layer system design along with different approaches, including the traffic assessment modeling and the development of control algorithms. This approach utilizes individual vehicle measurements, including individual vehicle speeds and time headways, as the major type of data for the system operation. A prototype of a CPC detection based queue warning system was developed by a research team at the University of Minnesota led by Dr. John Hourdos and is described in Chapter 2 of this report.

CHAPTER 2: DEVELOPMENT AND FIELD DEPLOYMENT OF A QUEUE WARNING SYSTEM ON I-94 WB BASED ON DETECTION OF CRASH-PRONE CONDITIONS

This report presents the design, specification, implementation, and evaluation of an infrastructure-based queue warning system (QWARN) that is capable of detecting dangerous traffic conditions, i.e., crash-prone conditions (CPCs), on freeways and delivering warning messages to drivers to increase their alertness in these traffic conditions and ultimately reduce the crash frequency on urban freeways. This effort approaches the topic from the quantification of traffic flow to the multi-layer system design along with different approaches including the traffic assessment modeling and the development of control algorithms. This report presents the QWARN system architecture and deployment and introduces a new approach to evaluating efficiency the proposed system that is not bound by the constraints of traditional evaluation indexes such as false alarm rate. This study utilizes measurements of individual vehicle speeds and time headways at two fixed locations on the freeway mainline as the main source of data for the system's operation. Finally, the report concludes with an evaluation of the proposed system implemented on a freeway section with a high crash frequency. The queue warning system was implemented in the right lane of a 1.7-mile-long freeway segment of westbound Interstate 94 (I-94 WB) near downtown Minneapolis where the event frequency prior to the system's installation was 11.9 crashes per million vehicles traveled(MVT) and 111.8 near crashes per million vehicles traveled(MVT). Machine Vision Detectors (MVDs) installed on a nearby rooftop captured the real-time vehicle data. The data were delivered to a server running the main control algorithm at the Minnesota Traffic Observatory (MTO) via MTO's communication network. The control algorithm assesses the "dangerousness" of the given traffic conditions and responds with a warning result based on a multi-metric traffic evaluation model and a control-reasoning heuristic.

2.1 STUDY SITE AND AVAILABLE DATA

To best study crashes, conditions must be observed and measured before, during, and shortly after an actual event. This requirement translates to a need for continuous monitoring and data collection at a location that maximizes the probability of capturing crashes on camera.

In the Minneapolis-Saint Paul Metropolitan Area (Twin Cities), I-94 connects the two cities and is the major freeway corridor connecting the two banks of the Mississippi River in the region. The site of this study is a segment with a length of 1.7 miles on I-94 WB near downtown Minneapolis. This segment of I-94 is near the exit of I-35W, the west branch of Interstate 35 that runs through Minneapolis. The close proximity to the downtown area results in a large traffic volume merging in and out these two freeways. The combination of such a large vehicle volume and great degree of merging often destabilizes traffic on this freeway segment thereby causing shockwaves where drivers need to reduce their speed in a short time and space or, when drivers fail to decrease their speed quickly enough, rear-end crashes. According to MnDOT records, this segment had the highest crash rate in the entire Minnesota freeway system. In 2002, the site exhibited 4.81 crashes per million vehicle miles (MVM) – equivalent to approximately one

crash every two days – while the network average is 0.96 crashes per MVM. During the PM peak period, the aforementioned site exhibited an average of 15.43 crashes/MVM whereas the entire I-94 freeway experienced only 3.29 crashes/MVM (81)]. Fatalities and severe injuries are very rare since the prevailing speed during CPCs is relatively low. The majority of crashes result only in property damage.

Figure 2.1 Aerial view of implementation site.

The crash-prone section of I-94 WB runs parallel to I-35W and short ramps allow transfers between freeways (Figure 2.1). The freeways and cross streets are labeled. The changeable message boards are denoted by the red circles and the high-volume on-ramp is enclosed by the green rectangle. The site includes two on-ramps, three off-ramps, three main lanes, and two 3,000-foot auxiliary lanes – one in each of the two areas where weaving is common (just downstream of the green rectangle and between the two red circles in Figure 2-1). Weaving is excessive where high volumes enter from the ramp (outlined by the green rectangle in Figure 2-1) which combines traffic from Minnesota State Highway 65 (MN 65) and the downtown business center to the north with I-94. In addition to the traffic volume entering the rightmost lane from the ramp, many drivers on I-94 merge right in order to be in or near the rightmost lane in anticipation of the two off-ramps downstream of Lasalle Ave. During periods of congestion, shockwaves generally originate when vehicles merge onto I-94 from the aforementioned ramp and cause vehicles in the rightmost lane to brake. If conditions are sufficiently dense, one vehicle entering from the ramp can initiate a chain reaction of vehicles braking that grows into a shockwave that causes increasingly intense braking as it moves upstream. Due to vertical and horizontal curves, vehicles between Chicago Ave and Portland Ave have limited forward sight distance. Drivers' inability to see a shockwave approaching forces them to rely heavily on their reaction time to avoid rear-ending the vehicle ahead of them.

In an attempt to reduce the number of shockwaves, a double white line was extended by 1000 feet from the point where the ramp joins I-94 to the region between 1st Ave S and Nicollet Ave. The intent was to prohibit merging for another 1000 feet in order to move the merging zone to an area with longer forward sight distances and make it easier for drivers on the ramp to match the speed of traffic on I-94. While this solution reduced the severity of the crashes, it did not reduce their frequency.

In 2002, for the purposes of projects related to intelligent transportation systems (ITS), a traffic detection and surveillance laboratory was established as part of the Minnesota Traffic Observatory (MTO) at the University of Minnesota. Hourdakis et al. (*22*) report details of the site instrumentation and

capabilities. Because the site is close to the downtown area, nearby high-rise buildings allowed for the installation of several cameras and MVDs overlooking the roadway. While most of the sensors are not utilized by the queue warning system, they provide the means of collecting detailed observations and determining ground truth.

As shown in Table 2-1, different types of data were used across this study. Individual vehicle measurements of speed and time headway were used for the operation of the system and aggregated traffic speed data from loop detectors serve for system adjustment and system evaluation. In order to collect the necessary individual vehicle data cost-effectively and unobtrusively, MVDs were utilized (Figure 2.2). Due to the high concentration of conflict events at the test site, only two such sensors stations were necessary, one placed at the location of the most frequent crashes (right) and the second approximately 750 feet downstream (left). The two stations were deployed between 3rd Ave and MN 65 and between MN 65 and Portland Ave.

Table 2-1 Summary of data types and purpose

Data	Type	Source	Purpose
Aggregated Traffic Data	Real-Time	Loop Detector	Additional input for system adjustment
Aggregated Traffic Data	Historical	Loop Detector	Developing of system evaluation methodology
Individual Vehicle Measurements	Real-Time	MVD	The main input of the system
Individual Vehicle Measurements	Historical	MVD	Algorithm and system design and development
Traffic Event Data	Historical	Video	System evaluation methodology development, algorithm and system development

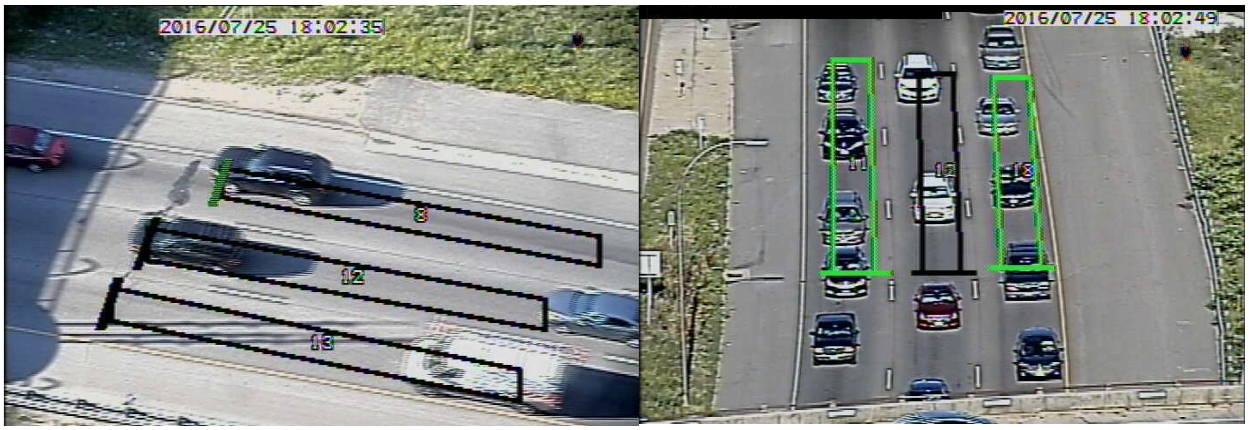

Figure 2.2 Machine Vision Sensors

This study also utilized MnDOT in-pavement loop detectors to provide 30-second volume and occupancy data to provide additional information for system adjustment from policy-makers. Five surveillance cameras were also employed: four atop a high-rise building to capture vehicle conflict events between 3rd Ave and Chicago Ave on video and one atop a pole to capture live video of the MnDOT changeable message boards at the 11th Ave gantry (rightmost red circle in Figure 2.1). Video from all five cameras was captured and saved digitally from 9 a.m. to 8 p.m. every day. Vehicle data from the loop detector is collected 24 hours a day, 7 days a week whereas the individual vehicle measurements were only collected between 7 a.m. and 8 p.m. each day. Traffic event data extracted from these surveillance videos were used to measure the performance of the proposed system in a real-world context.

2.2 TRAFFIC MEASUREMENTS AND METRICS

Several metrics are calculated using individual vehicle information such as speed and headway in order to quantitatively describe traffic conditions. While individual vehicle measurements hold the benefit of providing very high-definition data, they also carry large amount of stochastic noise. This fact brings about the paradox that although aggregation can reduce the impact of noise, it also results in loss of detailed information. Increasing the resolution to compensate for aggregation tends to cause more noise. Traditionally, individual vehicle measurements are aggregated in time to produce averages. While the time-aggregated data has less noise, it can no longer describe both the temporal and spatial nature of different traffic flow conditions.

In order to obtain detailed information without much noise, a multi-metric approach was utilized in this study to aggregate the data into different traffic metrics. This approach reduces the impact of noise by aggregating individual vehicle measurements over space and time while the combination of different metrics attempt compensates for the loss of information during the aggregation and quantifies more characteristics of the traffic flow. To that end, Hourdos et al. (4) proposed a series of traffic metrics derived from individual vehicle measurements, both temporal and spatial, to detect CPCs in freeway traffic. Variations of metrics were also introduced to reflect aggregation over time and space. These metrics include average speed, coefficient of variation of speed, traffic pressure, kinetic energy, coefficient of variation of time headway, coefficient of variation of space headway, acceleration noise, mean velocity gradient, quality of flow index, and a number of heuristic metrics calculated with data from multiple detectors.

Generally, a moving average window approach was utilized in this study to perform the translation from individual vehicle measurements to the aforementioned metrics. Given a sequence of individual vehicle speeds and their respective time stamps, the subset of data needed for the calculation of specific traffic metrics is selected based on the prior time shift and the size of the window. Window size represents the number of vehicles in a window. The prior time shift determines the location of the moving window and is determined by the length of time between the last vehicle in the window and the latest vehicle data collected in the real-time system. With these two parameters, a sample of speeds can be selected for the calculation. In this study, window sizes (in the units of number of vehicles included) were chosen from the set {15,30,40,50,60,70,80,100,110,120} and prior time shifts (in seconds) were selected from

the set {10,30,60,120,180,240,300}. The variations in temporal and spatial metrics that follow will be denoted in the form Metric-Location-Lane-Window_size-Window_end_time. For example, AvgSp-Down-R-15-30 denotes the average speed among 15 vehicles on the right lane of the downstream station at least 30 seconds ago.

2.2.1 Temporal Metrics

The following are the definitions of a few of the metrics used in the estimation of the crash probability.

2.2.1.1 Average Speed

Average speed is a common and informative statistic and helps reduce stochastic noise.

2.2.1.2 Coefficient of Variation of Speed (CVS)

In addition to averaging, standard deviation is also a popular way to account for data dispersion. The coefficient of variation, also called relative standard deviation, standardizes the actual standard deviation by its sample mean. The CVS is the product of the standard deviation and the mean value of the speed. As its definition implies, a higher value of the coefficient of variation of speed means higher variability in the speed data.

2.2.1.3 Coefficient of Variation of Time Headway (CVTH)

The time headway (TH) between vehicles is an important metric that describes safety and level of service. TH calculation requires individual vehicle arrival times at a point and is simply the difference between the arrival times of two successive vehicles. For the purposes of this research, the actual time headways are not as important as the magnitudes and rates of their change, so the chosen metric is the coefficient of variation of TH in a group of n vehicles.

2.2.2 Spatial Metrics

2.2.2.1 Density

Density (k) is defined as the number of vehicles per unit length of road. It is an important characteristic of traffic flow in many models describing its relationship with speed. There are several different models that measure density such as a linear model by Greenshields, a log model by Greenberg, an exponential model by Underwood, and many others. In this report, density is not used directly but rather as a component in the calculations of other traffic metrics such as traffic pressure and kinetic energy.

2.2.2.2 Acceleration Noise

Acceleration noise is a measure of the smoothness of the traffic flow based on an estimation of individual acceleration dispersion. Three factors are highly related to the value of acceleration noise:

driver behavior, road conditions and geometry, and traffic conditions. The calculation of the acceleration noise in this study follows the approximation proposed by Jones and Potts (23).

2.2.2.3 Mean Velocity Gradient

In order to differentiate between different traffic conditions with similar acceleration noise, such as slow, congested traffic versus fast traffic inside a shockwave, Helly and Baker (24) proposed another measurement, the mean velocity gradient, described by Equation 2.1.

$$MVG = \frac{\sum_{i=1}^{N}(MVG_i)}{N} \qquad (2.1)$$

$$MVG_i = \frac{(AN)_i}{\overline{u_i}}$$

Where

MVG: Average Mean Velocity Gradient

MVG_i: Mean Velocity Gradient of vehicle i

N: The total number of vehicles in a hypothetical mile

$(AN)_i$: Acceleration Noise

$\overline{u_i}$: Average speed (mean velocity) of vehicle i

2.2.2.4 Quality of Flow Index

The quality of flow index proposed by Greenshields (25) provides a quantitative metric to describe the safety of the traffic conditions on a given road based on the number of speed changes and their frequency (Equation 2.2).

$$QFI = \frac{\sum_{i=1}^{N} QFI_i}{N}$$

$$QFI_i = \frac{k\bar{u}}{\Delta u}\sqrt{f} \qquad (2.2)$$

Where

QFI : Average Quality of Flow Index

QFI_i : Quality of Flow Index of Vehicle i

N : Total number of vehicles in a hypothetical mile

$\bar{u}$: Average speed

Δu : Absolute sums of speed changes in a mile

f : Number of speed changes in a mile

k : Constant of 1000 when speed unit is mph and the length of the section is one mile.

2.2.2.5 Traffic Pressure

Traffic pressure (TP) was designed to measure the smoothness of traffic flow. It is defined as the product of speed variance and density (26) as seen in Equation 2.3a. A higher density is generally associated with a lower average speed. When both the density and the variance of speed are high, it may indicate a "stop-and-go" traffic that could be dangerous and crash prone.

$$TP = \sigma_s^2 \times k \qquad (2.3a)$$

Where

TP : Traffic Pressure

σ_s^2 : Speed variance

k : Density

2.2.2.6 Kinetic Energy (KE)

Kinetic Energy is a familiar quantity in the world of physics that represents the energy of a moving object. This measurement can also be modified to quantify the energy stored in the traffic flow. In the context of traffic flow, kinetic energy measures the energy in the motion of the traffic stream.

Similar to the concept of energy used in physics, the total amount of "energy" in a traffic system cannot change but can be converted to another form. Drew (27) described the antithesis of kinetic energy as internal energy or erratic motion due to the road geometry and vehicle interactions that corresponds to an earlier description of acceleration noise. Please note that the "kinetic energy" in this study is for traffic flow and is different from the kinetic energy of a moving object, which means it is not dependent on the mass of vehicles but instead on the density of the traffic stream. The formulation of KE is described in equation 2.3b.

$$KE = ak(\bar{u})^2 \qquad (2.3b)$$

Where

a : kinetic energy correction parameter, a dimensionless constant, here it is taken as 1

k : density of the traffic stream

$\bar{u}$: average speed of the stream

2.2.3 Heuristic Metrics

2.2.3.1 Up/Down Speed Difference

The up/down speed difference is the difference between the maximum vehicle speed at the upstream sensor and the minimum vehicle speed at the downstream sensor. Its purpose is to measure the travel behavior of a shockwave. For example, when traffic is smooth without shockwaves, the up/down speed difference should be small. When a shockwave has reached the downstream sensor, but has not yet reached the upstream sensor, there should be a lower speed downstream than upstream thus resulting in a high up/down speed difference. A positive up/down speed difference indicates that the maximum speed of upstream is higher than the minimum speed of downstream. On the other hand, a negative sign of up/down speed difference indicates that the maximum speed of upstream is lower than the minimum speed of downstream. The latter case may happen when upstream is congested and downstream traffic is already recovering from congestion.

2.2.3.2 Right/Middle Lane Speed Difference

As the name suggests, this metric is the difference in speeds between the right lane and the middle lane. When the traffic on the right lane is significantly slower than that on the middle lane, lane changes become more dangerous as they require drivers to divert their attention from the traffic ahead and search for a gap in their mirrors. This increases their reaction time which can be dangerous when shockwaves approach.

2.2.3.3 Max/Min Speed Difference

This metric measures difference between the maximum speed and minimum speed on a sensor location for a given prior time shift and window size. When a shockwave hits a location, in a relatively short

number of vehicles, the speeds tend to fluctuate and drop and results in a high Max/Min Speed Difference. Such high value is usually observed in the occurrence of traffic oscillations and crashes.

2.2.4 Individual Vehicle Speed Noise Reduction

All sensors inherently have error and noise in their measurements, and such noise can cause surges in the crash-likelihood calculation and compromise the accuracy of the model. In order to reduce the noise in a time series, filtering techniques such as the one proposed by Hourdos (28) in his development of a crash probability model are often employed. To perform a time series analysis and noise removal, the original unstructured speed data needs to be translated into a 1-second-speed time series using interpolation. Two different interpolation methods, linear interpolation and spline interpolation, were considered as candidates and tested in a preliminary study by the authors. Linear interpolation consists of simply connecting the data points with straight lines while spline interpolation uses a single, continuous curve to connect all the points. When comparing these two methods, spline interpolation was found to be problematic as the requirement that the data points be connected with a smooth curve produced interpolated speeds that were well outside of the normal range thereby introducing additional error and noise. Because of this issue with the spline interpolation method, linear interpolation was selected for this study. Of the several different filters that Hourdos designed and tested on their ability to remove impulse noise, his Digital FIR Hamming filter was selected to perform the noise reduction for the system.

After filtering, the data become another time series with lower noise. Given that the time headways between vehicles are as informative as their speeds, the dataset needs to be returned to its original form before the traffic metrics are calculated. A reverse interpolation method finding the filtered speeds at the times of the original data points is implemented.

2.3 CRASH PROBABILITY MODEL

Using the described metrics and their variants as well as the selected digital filter, a crash probability model was produced. The model is based on a fitted logistic regression model. The model described by Hourdos (28) was employed to determine the likelihood of a crash which is the main input in both the CPC detection algorithm and resulting queue warning system.

2.3.1 System Architecture

This section presents the system architecture. As shown in Figure 2.3, the system follows a three-layer design. The Crash Probability layer collects real-time individual vehicle measurements and processes them to remove noise. The filtered data then pass to the crash-probability model to assess the likelihood of a crash. This crash likelihood along with additional traffic information such as speeds and headways are passed to the second layer, the Algorithm layer. In this layer, the algorithm decides if a warning message should be generated by comparing the crash probability with preset thresholds and real-time traffic conditions. A decision of whether to raise or drop the alarm is being generated and

passed to the third layer: System Control, in which requirements from policy makers are applied to modify the result before delivering it to the message sign in the field.

2.3.2 Control Algorithm

This section describes the second layer of the system, the control algorithm. The control algorithm is developed to determine when to start and stop showing the warning message. The inputs to the algorithm are the crash probability and the filtered vehicle speeds. A moving median filter, or average filter, is applied to the crash probabilities to reduce noise and outliers. A dynamic average window methodology is used to calculate the adjusted crash probability for real-time traffic conditions. Based on this adjusted crash probability, user-defined thresholds, and the result of a speed test (see Equation 2.4), the decision as to whether to raise the alarm is made by the system. Once the alarm is raised, it remains active for a minimum of one minute regardless of whether the crash probability drops below the threshold. This assures that the sign will remain active throughout the trajectory of the shockwave that raised the alarm. Each subsequent alarm renews the one-minute extension.

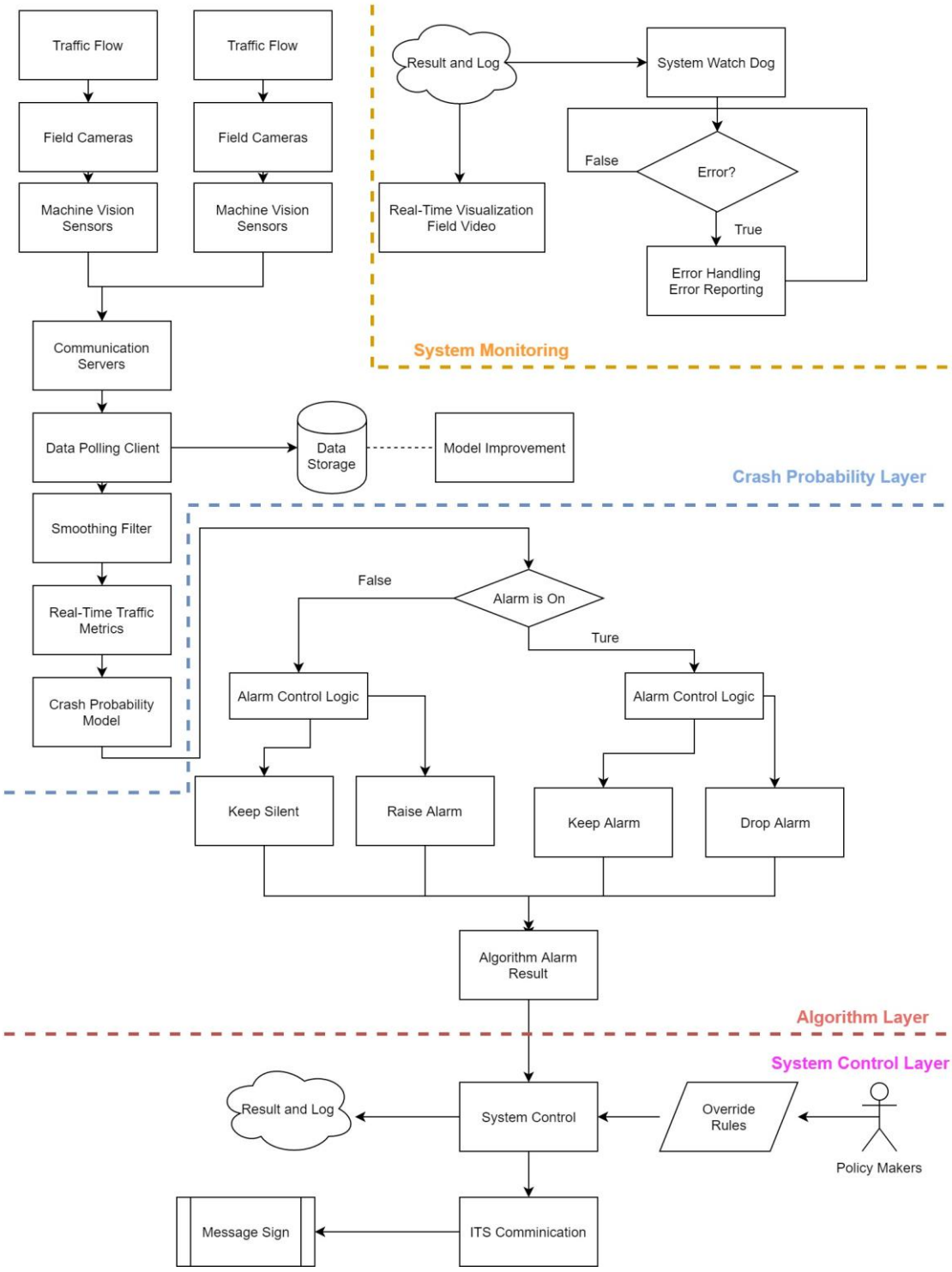

Figure 2.3 System Architecture

2.3.3 Control Logic

The crash likelihood alone is not sufficient for determining the precise time to warn the drivers while still producing consistent and stable decisions. Since the crash probability is a continuous variable, a two-threshold approach is employed to determine whether a crash likelihood indicates crash-prone conditions. One threshold for determining the raising of the alarm and a second for determining its termination. In addition to the crash probability, the algorithm proposed in this report also takes additional traffic measurements into consideration to increase the accuracy and efficiency of the alarm.

Once the alarm is initiated, it will remain active for a minimum time period, currently one minute. Since the individual vehicle data is inherently noisy and can change very quickly, the single model structure used to measure the crash probability can generate spikes when it encounters speed outliers. A spike in noise caused by outliers takes the form of a sudden surge in the value of crash probability and a sudden drop a very short time after the surge. The values before and after such spike were usually in similar ranges. Therefore, such a spike may activate the alarm trigger for only several seconds during which the alarm shouldn't be raised. Thus, deciding the status of the alarm based only by the alarm trigger can lead to frequent changing of warning messages. The control logic of the algorithm can be found below in Equation 2.4.

$$
\begin{aligned}
&Greater(\overline{p_t}, \lambda_1) \wedge SpeedTest(v_{tb}) \rightarrow AlarmOn \\
&AlarmOn \wedge Greater(\lambda_2, \overline{p_t},) \wedge TimeCheck(t) \rightarrow AlarmOff \\
&SpeedTest(v_{tb}) = \begin{cases} true & v_{tb} \le u_1 \\ false & v_{tb} > u_1 \end{cases} \\
&TimeCheck(t) = \begin{cases} true & t - t_0 > \Delta t \\ false & t - t_0 \le \Delta t \end{cases}
\end{aligned}
\tag{2.4}
$$

Where

u_1 : test speed, default is 45 mph. (mph)

t_0 : last time in the past with an alarm trigger (s)

λ_1 : Starting Threshold

λ_2 : Ending Threshold

v_{tb} : Current Downstream Speed (mph)

$\overline{p_t}$: Adjusted Crash Probability

$$\overline{p_t} = \frac{1}{n}\sum_{i=t-n+1}^{t} p_i \qquad n = \begin{cases} f(\overline{p_t}, \lambda_1) & \overline{p_t} \geq \lambda_1 \\ g(\overline{p_t}, \lambda_1, \lambda_2) & \lambda_2 \leq \overline{p_t} < \lambda_1 \\ h(\overline{p_t}) & \overline{p_t} < \lambda_2 \end{cases} \tag{2.5}$$

As shown in equations 2.4 and 2.5, the algorithm regards the crash probability as one of the inputs needed to decide whether to raise or lower the alarm. The adjusted crash probability is used instead of the direct output from the crash probability model. The value n is the size of the dynamic window used to average the crash probability. Using a dynamic window size makes the algorithm more sensitive to crash-prone conditions and reduces the probability of false alarms caused by noise in the measurement. The dynamic window size is calculated through three conditions, as described in Equation 2.5, with different results depending on which threshold it is nearest. The controlling hypothesis is that the noise in the crash probability will be higher around the selected thresholds so more samples are used to calculate the average unless the crash probability suddenly increases to values close to 100% in which case the averaging window is made much smaller in order to reduce the delay in raising the alarm.

Figure 2.4 MnDOT changeable message boards with warning displayed.

2.3.4 External Controls

As part of the terms for the deployment of the system, two overrides were included and the preexisting MnDOT signs' (Figure 2.4) refresh rate was kept. The two sets of changeable message boards used are fixed to gantries above the freeway. The overrides are intended to limit the possibility of overexposure of drivers to the warning by what was, at the time of implementation, an unproven system and consist of a time override and a congestion override. The time override prevents the sign from being turned on, regardless of the alarm status before noon or after 8 p.m. because MnDOT felt that traffic conditions at those times would be too prone to producing false alarms. The congestion override also prevents the sign from being turned on when five consecutive 30-second average speed measurements at the loop detector upstream of the farthest upstream sign are below the MnDOT-imposed threshold of 25 mph. This override is intended to reduce driver overexposure to the warning by not displaying a warning when drivers are already travelling slowly. The rate at which the sign is updated is a result of the sign being part of the MnDOT Twin Cities metro-wide network. Initial activation can vary from a few seconds to one minute, depending on the synchronization between the independent queue-warning system and the traffic operations system that controls the signs. This delay amplifies short gaps in the alarm activation (e.g. even if the alarm is only lowered for 10 seconds, the sign could be off for up to a minute).

2.3.5 Interface and Control Station

In order to allow the users of QWARN to monitor the system and traffic conditions in real-time, a live feed of the model result, MVD data, sign status, and cameras used for event detection is available during the system's operation. Although the actual application resides in one of the secure servers of the MTO, a station has been installed in the lab area that allows monitoring of all relevant feeds (Figure 2.5). The QWARN application has been developed to be able to operate from any kind of computer even in the Cloud. All communications are Ethernet based so any instance of the application that has the right credentials can poll the MVDs for data and produce the warning messages. At the moment, the application resides behind the combined firewalls of the University of Minnesota and the MTO.

The system has been developed to include several safety and redundancy features. For example, if for any reason, the actual application crashes, a separate watchdog application will attempt to restart it and, if that fails or the entire server is down, an alert email is dispatched to the MTO lab manager informing him of the situation. The integration with MnDOT's Regional Traffic Management Center (RTMC) IRIS traffic operations system is performed through a secure web connection that makes hacking into either system virtually impossible since IRIS is polling the QWARN application every 30 sec for a message instead of pushing messages to the traffic operations system. Messages are not dynamically selectable so even if a hacker could take control of the system the "Slow Traffic Ahead" message is the only one they would be able to display. Finally, each message IRIS receives has a 45 sec lifetime so if the warning has been raised and the system crashes the sign will turn off after 45 seconds to avoid cases where the warnings are still up when conditions are non-crash prone or the congestion override has been imposed.

A picture of the GUI of the QWARN system is presented in Figure 2.6. The upper left screen (shown in detail in figure 2-6) shows the status of the data feed from the MVDs, the last 60 estimations of crash probability (both raw and adjusted), the thresholds under which the system is operating, a continuously-updating plot of the model, the algorithm, and the override results, command line windows for the watchdog application, a feed from IRIS on the current status of the ILCS, and a feed of speed measurements from the loop detectors controlling the congestion override. The other screens show the various camera feeds and the video feeds from the MVDs.

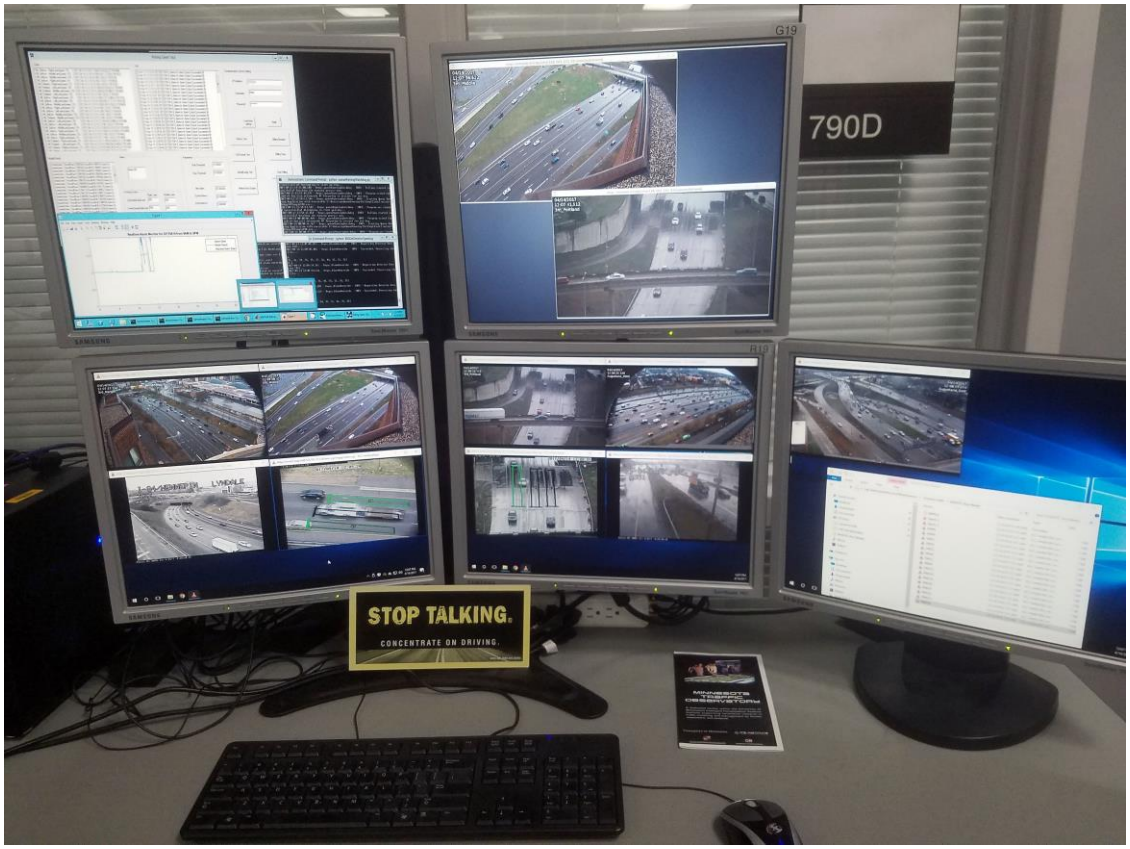

Figure 2.5 QWARN Monitoring Station at the MTO

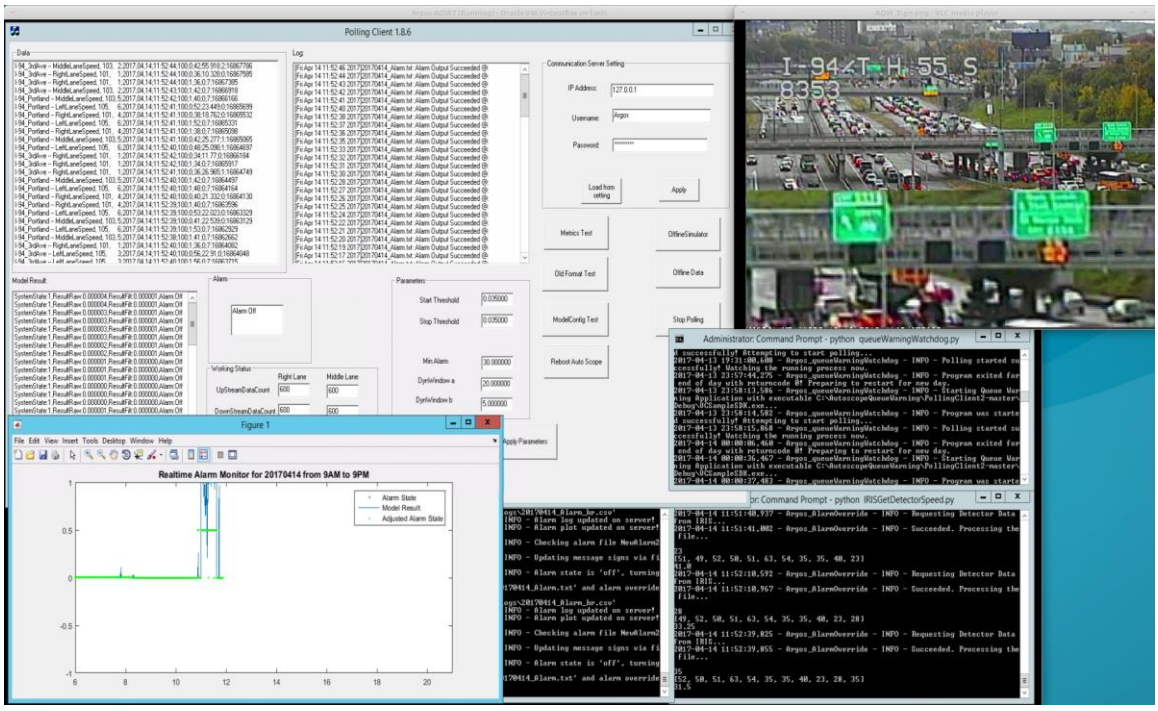

Figure 2.6 Detail of the User Interface of the QWARN System

2.4 SYSTEM CALIBRATION AND VALIDATION

2.4.1 Calibration Basics

Calibration is important to optimize the performance of a system with a number of user-defined parameters such as the thresholds for the crash probability model and the speed test. Calibration requires knowledge of the ground truth and a set of metrics for evaluating system performance.

In the context of Intelligent Transportation Systems, Automated Incident Detection (AID) systems were the first examples of real-time detection and alarm traffic operations tools. Inevitably, those systems' characteristics influenced and shaped the definitions of performance metrics for this type of real-time application. The performance criteria focused on the efficiency, accuracy, and robustness of such systems. For AIDs the important factors were to generate an alarm as soon as possible after an incident event happened and to not generate alarms when no such incident event has taken place. These two objectives target accuracy both in terms of generating alarms for as many, if not all, of the events, as well as reducing alarms raised where no event has happened. Efficiency metrics targeted AID performance in minimizing human operator effort spend on false alarms. The accuracy metrics include the false alarm rate (FAR) and detection rate (DR), while the metric targeting efficiency is false decision rate (FDR). In the context of AIDs, the FAR is usually the number of alarms raised when no incident was present divided by the total number of alarms generated while the system was running. The DR is the

number alarms raised when an incident happened divided by the total number of incidents occurred while the system was in operation. The FDR is the combination of the missed-detection rate and false alarm rate. Detection systems are required to decide whether to raise the alarm at each time interval they operate on. FDR is the sum of all intervals that the system raised the alarm for but no incident existed and the intervals were an incident was present but the system did not raise the alarm, all divided by the total number of intervals the system was in operation. High DR and low FAR and FDR are preferred describing an accurate and efficient system. A tradeoff between FAR and DR is a common issue in such systems. An overly sensitive system may have a very high DR, but by being sensitive, it can raise the alarm while nothing happened, resulting in a high FAR.

Unfortunately, the aforementioned performance metrics, as defined, are not suitable for the evaluation of a CPC detection system like the one described in this report. When discussing these metrics, it is important to note that the objective of AIDs is to detect an event that has happened and alert operators so they can initiate the process of incident response and clearance. AIDs did not interact with the drivers and did not aim in changing driving behavior to avoid the event that were designed to detect. The CPC detection system presented in this report is a crash prevention system which implies the following:

- CPC detection systems aim to detect conditions that may lead to a crash but have not done so yet.
- Warn drivers that are about to encounter CPCs and help them navigate such unsafe conditions.
- Warning the drivers can also change driver behavior enough to eliminate the CPCs themselves.
- An AID raising the alarm when no incident happens is a clear failure whereas a CPC detector raising the alarm and nothing bad happening could mean failure if the conditions were not crash prone but it could mean success if a potential crash was avoided.
- Incidents are factual events and in extent the detection of their existence is a binary, true or false situation. The causal factors precipitating to a crash, as described in Hourdos et. Al. (4), include the traffic conditions described as crash prone but, more importantly, involve factors related to the individual drivers such as reaction time, awareness, distraction, etc. The same CPCs can result in a crash if a distracted driver is involved or no crash or a near-crash if all drivers involved are attentive.
- CPCs are traffic conditions where the probability of a crash is higher than normal, there is no objective way to definitively classify a time period as crash prone where no crash or near-crash has happened.

Using the aforementioned performance metrics as defined to judge the system proposed in this report can result on overly conservative results and a calibrated system of much lower performance than the one possible to achieve. Therefore, there is a need for a more robust and leveled performance metric. Towards that effect, this study proposes a new metric, the Alarm Efficiency Score (AES), that better fits the nature of a real-time driver warning system. The AES is calculated based on the historical crash likelihood score and the alarm results of the day on which the system performance is to be evaluated. Unlike the FAR, the AES is not in a percentage scale. Therefore, in terms of calibration, it only has meaning when comparing two or multiple results produced by different systems or the same system with different parameters. A higher AES indicates a better performance.

2.5 HISTORICAL INCIDENT LIKELIHOOD SCORE

This study utilized the historical event likelihood approach to measure how dangerous a traffic condition can be. Given a certain time on a historical day, the similarity of the traffic condition during that time was compared with the traffic conditions when events happened and calculated a likelihood of an event.

2.5.1 Representation of Traffic Condition

For representing traffic states, two separate ten-dimensional spaces, one of volume and one of occupancy, were defined. Each traffic condition is represented by a set of these ten-dimensional vectors. Equation 2.6 is an example of the vector of volume at time t. The value of the 10th dimension equals to the volume at time t.

$$vec_{vol}(t) = (vol_{t-9}, vol_{t-8}, vol_{t-7}, vol_{t-6}, vol_{t-5}, vol_{t-4}, vol_{t-3}, vol_{t-2}, vol_{t-1}, vol_t) \quad (2.6)$$

Where

$vec_{vol}(t)$: The volume vector at time t;

vol_t : The volume at time t;

t : Time, in this case t is the number of the 30s segment;

The volume and occupancy data from loop detectors were aggregated over 30-second intervals forming 30-second-long time segments. The time variable, t, is equal to the number of the time segment. This study uses loop detector data for convenience, but individual vehicle measurements can also be used as long as they are aggregated to represent stable traffic flow over time.

2.5.2 Data Normalization

The natural distributions of volume and occupancy are different. In order to convert them into the same metric, the data are normalized and representation vectors are created. The normalization function is described in Equation 2.7. The normalization process involves subtracting the mean from volume data and then dividing by the standard deviation. The normalization for occupancy is the same as for volume.

$$vol_i' = \frac{vol_i - \frac{1}{n}\sum_{i=1}^{n} vol_i}{\sqrt{\frac{1}{n}\sum_{i=1}^{n}(vol_i - \frac{1}{n}\sum_{i=1}^{n} vol_i)^2}} \quad (2.7)$$

Where

vol_i' : Normalized volume for time segment i;

vol_i : Original volume for time segment i;

n: Total number of time segment;

2.5.3 Similarity

This study uses similarity between a given traffic condition vector and all the condition vectors that precipitated crashes and near crashes to assess the "dangerousness" of a traffic condition. The assumption is that if a given traffic condition is very similar to the majority of traffic conditions corresponding to crashes and near-crashes, the given traffic condition is likely to be dangerous, too.

There are many similarity measurements such as cosine similarity, Euclidean distance, and extended Jaccard similarity. In this study, different types of similarity metrics were tested. Here, cosine similarity is chosen to demonstrate the evaluation methodology. Cosine similarity measures the angle of two high-dimensional vectors to determine their degree of likeness. As shown in Equation 2.8, the nature of cosine similarity makes it settle in the range (-1,1) with 1 representing the highest similarity.

$$\cos(\vec{A}, \vec{B}) = \frac{A*B}{\|\vec{A}\|\|\vec{B}\|} \quad (2.8)$$

Where *A, B* are two traffic vectors.

2.5.4 Modeling Crash Likelihood

To evaluate the validity of a model-produced crash likelihood for a given traffic condition, the main objective is to model the similarity of a given traffic condition compared to those known to be associated with crashes and near crashes.

Traffic measurements leading up to each historical event were extracted and used to formulate a set of historical traffic crash-prone conditions. Given a current traffic state represented in the two-vector approach, the similarity between the historical crash-prone conditions and the current conditions can be calculated to measure the comprehensive similarity of the two. Based on the assumption that a higher similarity between a given traffic condition to conditions that resulted in a crash corresponds to a higher probability of a crash, the likelihood of a crash can be estimated. Extending this concept to each day in the set of historical days used to evaluate the crash probability model, a map containing the similarity of each time period to the periods corresponding to historical events (crashes and near-crashes) can be constructed for each such day.

This map of similarities describes the dangerousness of traffic conditions for each target day. The values in the map, the crash likelihood score, are produced using Equation 2.9 in which L is the crash likelihood score, $V_{d,t}$, is the volume for traffic condition in day, d ,at time t; $V_{i,t}$ is the volume of event, i, at time t. Similarly, O represents the occupancy. This score will be different when the sample of historical crashes and near crashes is changed. Although it is not a percentage probability, it can quantify the dangerousness of different traffic conditions in that a higher score denotes more dangerous traffic conditions as compared to similar conditions that did not result in a crash or near crash. This approach provides the means to more fairly evaluate the queue warning system even with crash-prone conditions that may not involve reckless or inattentive drivers. Figure 2.7 shows the values of the crash likelihood score during a target day.

$$L_{i,t} = \sum_{n} (\mathrm{Cos}(V_{d,t}, V_{i,t}) \times \mathrm{Cos}(O_{d,t}, O_{i,t}))$$

$$\mathrm{Cos}(A, B) = \begin{cases} \mathrm{Cos}(A, B) & \mathrm{Cos}(A, B) > 0 \\ 0 & else \end{cases} \quad (2.9)$$

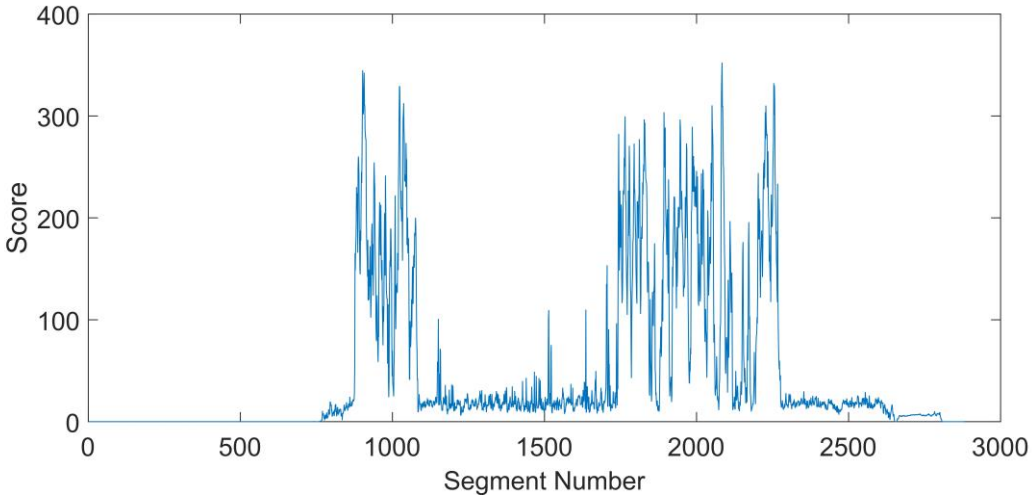

Figure 2.7 Crash Likelihood Score for a Target Day

2.5.5 Alarm Efficiency Score

The alarm efficiency score is a measure of how efficiently a warning system operates over a period of time. Equation 2.10 shows the mathematical formulation of the score. There are two components in the equation - the first measures the efficiency of all of the active alarms and the second serves as a penalty term for not warning about dangerous conditions. For an efficient queue warning system, it is desirable to cover as many dangerous traffic conditions as possible in the process of minimizing the total warning duration.

Assuming the evaluation period is a day, the first term in Equation 2.10 becomes the summation of crash likelihood score for all traffic conditions with the alarm being up, divided by the time that the alarm is up for this day. The first term is a density of historical crash likelihood approach and favors the system cover more crash likelihood score with a short alarm duration. Similarly, the second term becomes the summation of crash likelihood scores for all traffic conditions during which the alarm was down divided by the time that the alarm is down for the day.

$$E = \frac{\sum_{t_{on}} L_{ON}}{t_{ON}} - \frac{\sum_{t_{OFF}} L_{OFF}}{t_{OFF}} \quad (2.10)$$

L_{ON}: Likelihood score during alarm was up.

L_{OFF}: Likelihood score during alarm was down.

t_{ON}: Amount of time the alarm is on.

t_{OFF}: Amount of time the alarm is off.

Given different pairs of alarm activation and deactivation thresholds for the crash likelihood, different alarm efficiency scores can be calculated for the result of each of these threshold pairs as a means to compare their performances. Figure 2.8 shows a plot of the alarm efficiency score for different pairs of thresholds from {0.2,0.1} ({Start Threshold, Stop Threshold}) to {0.9,0.8} with a step of 0.1 for each threshold.

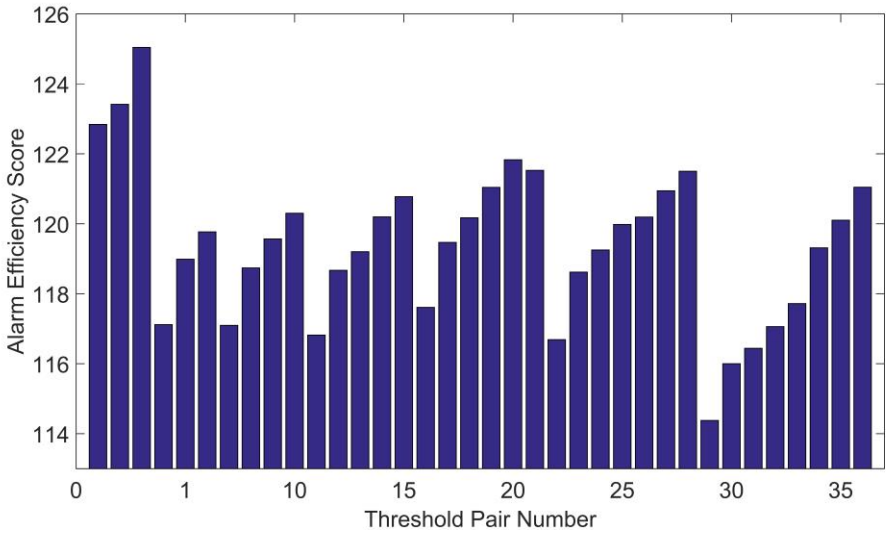

Figure 2.8 Alarm Efficiency Score for Different Sets of Thresholds

2.6 RESULTS AND DISCUSSION

The aim of this queue warning system is to efficiently alert drivers of CPCs they are about to encounter. The threshold for the crash probability used was among those proposed in in Hourdos et. Al. (4), for the speed data filter selected. The system operation was monitored during the three phases of the field implementation. Phase 1 lasted from March 1st, 2016 to April 30th, 2016 and involved the operation of the system in silent mode, meaning the sign was not activated but alarms where recorded. During this phase, the system's ability to operate correctly and reliably were tested and minor adjustments were

made in the system parameters. Phase 2 lasted from May 1st, 2016 to June 1st, 2016 and involved full system operation as well as the introduction of a heuristic test to reduce the time it took the alarm shut off at the end of the day when traffic returned to free-flow for the day. Phase 3 lasted from June 2nd, 2016 to August 31st, 2016 and involved the full operation of the system with no further changes or fine-tuning. The results presented in this report are those gathered during Phase 3.

In order to obtain the ground truth on which the system was to be evaluated, event observations were collected during Phase 3. This involved manual reduction of video from multiple cameras recording crashes and near-crashes that took place as well as recording the exact times the sign changed states. The data of 55 weekdays with sufficient video footage in this period were used to establish the ground truth. Some weekdays were excluded due to corrupted video files or equipment maintenance. Based on the ground truth established, detection rates under different system conditions were calculated. The false alarm rate, however, is much more difficult to calculate. Unlike the detection rate where the system performance is only evaluated at the time of an event, the only way to compute a false positive or false negative rate would be to go through the ground truth (the collected video) to determine if conditions were, in fact, crash-prone when the system said they were and calculate the false positive and false negative rates from that. Not only would it be extremely time-consuming to delineate all of the times when conditions appeared crash-prone, the task of labeling traffic conditions would be extremely subjective and therefore, unreliable. As such, no quantitative measure of the system's false alarm rate is available at the moment.

2.6.1 Detection Rates

To assess the performance of the system, the detection rate of all conflict events between 3rd Ave and Chicago Ave during the three-month evaluation period was calculated separately for the control algorithm and for the system as a whole. The detection rate was calculated for just the crashes, near crashes, and both events combined. To find the actual number of conflict events, all the events observed during the evaluation period were tabulated and sorted based on whether the drivers involved were warned or not warned about CPCs before the event and if the drivers were not warned, the events were separated by the reason the system failed to warn them (the results are tabulated in Table 2-2).

Table 2-2 Breakdown of system performance in right lane by component

Reason For Failure to Warn Driver	Event Type					
	Crashes		Near Crashes		All Events	
	[Count]	[% of Tot.]	[Count]	[% of Tot.]	[Count]	[% of Tot.]
Driver warned	15	36.6%	70	49.0%	85	47.3%

System buffering or inoperative	3	7.3%	8	5.6%	11	6.0%
Alarm was not raised	9	22.0%	28	19.6%	37	20.1%
MnDOT congestion override in place	8	19.5%	10	7.0%	18	9.8%
MnDOT time override in place	4	9.8%	25	17.5%	29	16.8%
System delay	2	4.9%	2	1.4%	4	2.2%
Total	**41**		**143**		**184**	

It is apparent that the control algorithm is far more successful at raising the alarm for events than the system as a whole is at activating the sign. As seen in Table 2-3, following a successful detection by the control algorithm, the main reason the sign was not activated is the presence of a MnDOT override.

Using the results shown in Table 2-2, the detection rates were calculated. To assist the reader in comparing the different detection rates and to measure the effect the overrides had on system performance, the results are separated in two categories; one is based on the algorithm decision and the other is based on the whole system which includes the algorithm, the overrides, and the sign refresh rate. In addition, these results are grouped into two categories based on time period; one for the full time that surveillance data were available (9 a.m. to 8 p.m.) and the other for the system operational period of noon to 8 p.m. during which the system was fully functioning. The results are tabulated in Table 2-3 which shows the rates at which various event types were detected by the algorithm and the rates at which the system as a whole provided a warning to the drivers involved in those events for the entire day and for just the time the MnDOT time override was not imposed.

Table 2-3 Detection rates during the evaluation period

Detecting Component	**Event Type**		
	Crashes	**Near Crashes**	**Both**
	[%]	**[%]**	**[%]**
Algorithm (9 a.m. to 8 p.m.)	76.3	79.3	78.6
Whole System (9 a.m. to 8 p.m.)	39.5	51.9	49.0
Algorithm (noon to 8 p.m.)	73.5	74.6	74.3
Whole System (noon to 8 p.m.)	44.1	63.6	59.2

Table 2-4 Event frequencies per million vehicles traveled (VMT)

Observation Zone	MN 65 to Portland Ave		3rd Ave to Park Ave
Observation Year	**2013**	**2016**	**2016**
Crashes	11.9	9.34	19.5
Near Crashes	111.8	51.8	93.0

Table 2-4 shows the frequencies at which events occurred in any lane between 9 a.m. and 8 p.m. on weekdays in June, July, and August of 2013 and 2016. The 2013 study only recorded crashes that occurred between MN 65 and Portland Ave whereas the 2016 study included a larger area. For comparison's sake, the 2016 events that occurred in the same region as the 2013 events are reported as well as the totals. Due to such expansion of the observation area for the 2016 study, crashes were observed at a greater frequency in 2016. However, when the events occurring outside of the observation zone used in 2013 are excluded from the 2016 data, it becomes apparent that there was a 22% decrease in crashes and a 54% decrease in near crashes in that zone following the implementation of the queue warning system.

Table 2-5 shows the average number of vehicles passing under the MN 65 bridge per day in 2013 and 2016. The change in the average from 2013 to 2016 is also reported in this table. It is interesting to note that the total Average Daily Traffic (ADT) decreased by roughly 5% between 2013 and 2016. The morning congestion observed in 2016 was not observed in 2013. During the time between the collection of the base data and the time the system was put in place, the timing of the traffic lights at the intersection of the on-ramp and 11th Ave was altered in order to reduce ramp spillback and reduce queuing in the right lane. That can be a reason for the morning congestion downstream but it doesn't necessarily account for the 5% drop. The effects of these changes in traffic patterns are uncertain.

Table 2-5 Average daily volumes during historical and current studies

Time Range	2013 Average	2016 Average	Percent Difference
9 a.m. to 8 p.m.	45260	42828	-5.4%
Whole day	74070	69758	-5.8%

2.6.2 System False Alarm Rate

A prominent concern when implementing the system was minimizing overexposure of drivers to the warning sign. This concern is what prompted MnDOT to impose what, in hindsight, turned out to be somewhat excessive congestion and time overrides. Of all types of overexposure, the case of a driver seeing a warning about slow or stopped traffic but not having to slow or stop is the one that must be avoided the most. Because the transition from crash-prone conditions to free-flow conditions usually occurs very suddenly (less than two minutes), the crash likelihood model has a tendency to continue

outputting crash probabilities indicative of crash-prone conditions for up to 15 minutes after uncongested flow conditions have been restored. In order to reduce the false alarm rate coming from this delay, an override was built into the control algorithm to deactivate the alarm, regardless of the model result at the time, when both MVDs observe 10 consecutive vehicles with speeds greater than 30 mph.

2.6.3 System Limitations

Due to the fact that the system is still in the prototype phase, several aspects of it are less than ideal and result in uncertainties of varying degrees. The limitations and uncertainties include the non-ideal configurations of the MVDs and warning sign, the limitations of the hardware, the fact that some of the equipment was shared with MnDOT, and the fact that the model result is currently computed for only the right lane. In the interest of cost and time, the MVDs were installed on a high-rise near the road rather than on a gantry or bridge directly over the road. The warning messages were displayed on the relatively small MnDOT changeable message board rather than a purpose-made display with potentially different characteristics (location, size, color, etc.). The limitations of the hardware also presented a source of uncertainty in that the speed data from the MnDOT single loop detector was only a 30-second average and was not completely accurate. Issues with power outages and lack of sufficient data storage at the rooftop station resulted in missing video data. Because control of the sign and the camera monitoring was shared with MnDOT, the sign was occasionally used to display incident management messages from MnDOT rather than the queue warning messages. Because the capability of the system to function as intended and the effect that it would have on drivers were unknown at the time of installation, it was only applied to one of the three lanes. As a result, it is unclear what effect this partial deployment had on driver's actions.

2.7 CONCLUSIONS

Impressions from the 55 weekdays of evaluation in the summer of 2016 suggest that the queue warning system prototype discussed in this report represents a successful crash prevention solution. The effect of the system on conflict events is difficult to determine from the data available but the system performs well given the constraints under which it is operating. The system raised the alarm for 79% of all conflict events that occurred during the evaluation period but was only able to warn drivers for 49% of all conflict events predominantly due to the overrides that were put in place to prevent the possibility of the system displaying the warning for excessive amounts of time. Why these crashes happened even with the drivers exposed to the warning is unknown. One can speculate that the message is not clear or strong enough. A lot of the vehicles involved are only exposed to the warning once on the Park Ave gantry since the warning sign further upstream is not visible from the entrance from 35W SB. The project was supposed to test different messages but due to time delays at both ends this did not happen. Regardless, if more messages were tested in the same period it would have been difficult to gauge the driver response since events are still infrequent and random.

Now that proof of concept has been confirmed, the next step will be to expand and optimize the infrastructure used by the system. Several changes to the system on the policy and infrastructure levels have been identified that will likely result in greater detection and warning rates and thereby decreased conflict event rates. Given greater design control, many of the system limitations could be mitigated if not eliminated altogether. This will include installing MVDs or other sensors on gantries or bridges directly above the freeway in so they are afforded a stable head-on view of traffic and placing the warning sign in a location selected by choice rather than necessity. The warning sign shape, size, location, and message may also need to be optimized to increase driver attention. The most important improvement will be expanding the system to all three lanes of traffic and following that change with a long-term study of the effects of the system on conflict event frequencies.

CHAPTER 3: DEVELOPMENT AND FIELD DEPLOYMENT OF A QUEUE WARNING SYSTEM ON I-35W SB BASED ON FREEWAY QUEUE LENGTH ESTIMATION

3.1 PROJECT MOTIVATION

Past research studies have shown that freeway rear-end collisions tend to occur in extended stop-and-go traffic or at end-of-queue locations (29). By identifying these kinds of traffic conditions and providing warning messages to drivers before they encounter those conditions, drivers are more alert of and prepared for crash prone conditions (CPCs) thereby reducing the likelihood of traffic accidents. This, in turn, improves mobility because severe traffic congestion caused by traffic accidents can be avoided or alleviated. This project holds the potential to improve both traffic safety and mobility.

3.2 PROJECT OBJECTIVES

The project objectives are:

1. Capitalize on past research and existing and new traffic detection capabilities on I-94 and new instrumentation on I-35W to develop a CPC detection system capable of generating alarms when the danger for rear-end collisions is high.
2. The project will evaluate potential driver warning messages that can be displayed by the existing intelligent lane crash signal (ILCS) and select the ones that are most effective in raising drivers' attention levels.
3. Finally, the project will develop a working prototype for the Rear-End Collision Prevention Driver Warning system and assist Minnesota Department of Transportation (MnDOT) in field implementation and testing.

3.3 LITERATURE REVIEW

3.3.1 Literature Review on Freeway Queue Length Estimation

Real-time prediction of the length of queues on freeways is of great help for the development of advanced freeway traffic management systems. Since the 1960s (42, 66, 76, 45), the importance of managing vehicle queue length to reduce vehicle delay and prevent spillover, especially at signalized intersections, has been recognized and studied (39, 40, 31, 62, 63, 35, 65).

3.3.1.1 Basic Methodology on Queue Length Estimation

Essentially, two basic approaches have been developed to estimate queue length, namely the cumulative traffic input-output methods and the shockwave methods.

The first type of queue length estimation model is based on the analysis of cumulative traffic counts at both the input and output to a link (30, 33, 43, 66, 68, 69, 70, 73, 74, and 75). Such models are commonly used to describe the traffic queuing process. However, according to Michalopoulos et al. (64), they are not sufficient for "obtaining the spatial distribution of queue lengths in time". Another obvious limitation of such models is that they are only able to estimate the queuing state when the queue length does not pass beyond the input detectors. These drawbacks limit the application of such type of models.

The second type of model analyzes vehicle queues based on the feature of traffic shockwaves. The shockwave analysis takes the traffic flow as a continuous flow on road and studies its characteristics. A shockwave, also known as the kinematic wave, is the interface between any two traffic states with different characteristics (flow rate, speed and/or density). The shockwave theory provides a powerful tool for analyzing the evolution of traffic condition in a time-space diagram, especially during the formation and dissipation of queues at highway bottlenecks. One of the main components of shockwave analysis is the traffic flow model selected. Lighthill and Whitham (56) and Richards (67) independently developed the first dynamic traffic flow model. Their namesake Lighthill Whitman Richards (LWR) model describes traffic on a link using a conservation law and an equilibrium relation between density and flow better known as the fundamental diagram (FD). Kinematic wave models have been widely used to study traffic dynamics on road links both analytically and numerically. Later, the original LWR model was extended in different directions to incorporate more realistic details. A more complete review of the traffic flow model and shockwave analysis was conducted by Maerivoet and De Moor (61).

3.3.1.2 Recent Work on Vehicle Queue Length Estimation

In particular, this section will review a number of recent works on vehicle queue analysis for intersections and freeway bottlenecks.

On the intersection vehicle queue estimation side, Hiribarren and Herrera (49) proposed a real-time traffic state estimation model utilizing vehicle trajectory data. Similarly, Cheng et al. (37) proposed a method of queue length estimation for signal control using sample vehicle's trajectories. Instead of using a traffic flow model, Comert and Cetin (38) developed a queue estimation method based on conditional probability and Bayes' rule.

Regarding vehicle queues on freeways, a great deal of work has been done on the queue analysis at freeway work zones. Jiang (52) applied shockwave analysis to estimate traffic delay and vehicle queue length at freeway work zones. Karim and Adeli (53) computed the queuing delay and vehicle queue length using a deterministic traffic flow model after calculating the freeway work zone's capacity. Later, Ghosh-Dastidar and Adeli (44) presented a microsimulation model based on a neural network for the queue length estimation at freeway work zones. A more comprehensive review on vehicle queue length estimation at freeway work zones was conducted by Weng and Meng (77). Beyond the vehicle queue analysis at work zones, Wu et al. (79) estimated queue length on freeway on-ramps. Similarly, the Kalman filter method was applied in Sheu et al. (71) to estimate real-time delays and queues in the presence of freeway incidents.

3.3.1.3 Vehicle Queue Length Estimation Methods Using High-Resolution Data

Regarding the data used to estimate vehicle queue, most of the researches use aggregated data. For instance, Skabardonis and Geroliminis (72) proposed a method to estimate intersection queue length using aggregated loop detector data in 30-second intervals. Some use probe vehicles' trajectory data, as presented above however, few of them fully utilized the high-resolution data. This is partially because the high-resolution traffic data was not available until recently.

Using the high-resolution event-based field data obtained from the SMART-Signal system, Liu et al. (58) developed a real-time queue length estimation method for congested signalized intersections. One of the appeals of this method is that it is capable of estimating the length of queues that exceed the location of upstream queue detectors. In particular, the high-resolution data was used to identify the "break points" (time and location of traffic flow pattern changes) which contributed significantly to the estimation of long queues. When the simple shockwave theory was applied to study the dynamics of traffic flow, field tests showed an accurate outcome from this method in terms of queue length estimation at intersections. As an application of this method, Liu and Ma (57) proposed a virtual vehicle probe model to estimate the time-dependent travel time. Though the objective was to estimate the travel time, queue length at the intersection was estimated in advance in order to accurately calculate the vehicle probe's travel speed. The field test on a corridor along France Avenue in Minneapolis, MN with 11 intersections demonstrated that the proposed model can generate accurate time-dependent travel times under various traffic conditions.

Based on these previous studies, a shockwave profile model (SPM) for traffic flow was proposed in Wu and Liu (80) which filled the research gap of implementing traffic flow model in signalized urban arterial. The SPM model is particularly suitable for simulating traffic flow on congested signalized arterials especially with queue spillover problems where the steady-state periodic pattern of queue build-up and dissipation process may break down. Field tests of the SPM model show that it can successfully identify the queue length, queue spillover occurrences and the dynamics of the vehicle queue for an arterial on TH-55 in Minnesota with three intersections.

However, it is not straightforward to extend the queue estimation algorithm from arterial to freeway. First, most queues on arterials are caused by traffic signals. They have fixed cyclical pattern that starts from a stop line at the beginning of a red period. Therefore, if the signal status is available, the onset of the queue can be immediately detected by a stop bar detector. A similar pattern exists for queues on freeway on-ramps (79), but it cannot be anticipated on freeway mainlines. The start of a stopped queue on freeways is not predictable; it can be anywhere at any time (41). Second, the speed of discharge shockwave is almost constant for a specific approach of an intersection, because the traffic state downstream of the queue at the beginning of discharge is always empty (58). On the other hand, freeway queues may begin to discharge under various downstream traffic conditions. Last, the impact of lane changes can be omitted for queues on arterials because vehicles are not permitted to change lanes when getting close to intersections. However, for most freeway segments, vehicles can change lane as long as they do not impede others.

3.3.1.4 Concluding Remarks

From the review above, it was found that most of the previous research focused on vehicle queue length estimation at signalized intersections and specific locations (e.g., work zones and ramps) on freeways. Fewer studies have been dedicated to the more general analysis of freeway vehicle queues. The lack of research on the theoretical analysis of freeway queue formation, evolution, and dissipation using high-resolution data is even more obvious. The difficulty of capturing the dynamics of freeway traffic maneuvers is one obstacle facing such analysis. Another difficulty is the lack of field data, especially high-resolution data. Realizing the research gap and the opportunity, developing methods to identify the freeway vehicle queue's formation, evolution and dissipation processes using high-resolution data collected from this project will contribute significantly both in theory and in practice.

3.3.2 Literature Review on Intelligent Lane Crash Signal

In the case that a queue on freeway is identified/predicted, informing drivers about the downstream queue and preparing them for the changes of traffic status will be helpful for freeway traffic management. In this project, ILCS are utilized to display warning messages and guide drivers to adjust speed to avoid potential rear-end collision and improve the freeway performance. In the following, the effectiveness of freeway ILCS systems and the response from drivers to such systems, both from simulation results and field tests, are reviewed.

3.3.2.1 Simulation and Survey Studies

Chatterjee et al. (36) conducted a survey on drivers' response to variable message signs (VMS) in which it was found from the questionnaires that only 1/3 of drivers saw the information and 1/5 of them would change their route choices. Many research works reported that drivers' behavior could be more influenced by speed advisory and lane changing signs (compared to the route-changing messages). For instance, Hassan et al. (48) investigated drivers' responses to different VMS messages with driving simulation software and concluded that the message of "Caution-fog ahead-reduce speed" was the one with the best effect.

Khan (54) developed an infrastructure-based queue-end warning system which automatically estimates the queue length and displays messages on portable VMS in order to reduce rear-end collisions. However, the exact messages on boards were not specified. This system was tested through driving simulators. It should be noted that because the warning system was deployed at freeway work zones, the location of the front of the queue was known. Whether the developed approach can handle other forms of queues on freeway is not clear. Lee and Abdel-Aty (55) conducted a study including 86 participants who drove a 5-mile section of freeway on a driving simulator. The participants were exposed to warning messages as well as speed limit messages. Simulation results showed that when warning messages or speed limits were displayed, participants generally drove at a uniform speed. Their research findings also indicated that warning messages were beneficial in reducing speed variation and removing congestion and could potentially reduce crash risk on freeways.

3.3.2.2 Examples of Real ILCS System Implementation

In addition to simulation and survey studies, field tests of variable message systems were also conducted. A large-scale real-time driver warning system called the Caltrans Automated Warning System (CAWS) was installed on Interstate 5 and State Route 120 near Stockton, California and was brought on line in 1996 (59, 60, 34, 46). CAWS displays various messages and signs to inform drivers about the approaching traffic conditions and the advised speed. Messages are designed for conditions with different visibilities and purposes. By comparing the data from both the study direction (the direction of freeway without warning system, I-5 North) and the control direction (the direction of freeway with a warning system, I-5 South), it showed that the number of crashes was reduced after the installation of the warning systems. Wrapson et al. (78) studied the effectiveness of different types of signs. By measuring the vehicle speed in a 50 kph zone, the study suggested that simply displaying the average speed of neighboring vehicles without giving a specific speed advisory or warning the drivers that their speeds were being measured could significantly reduce the vehicle speed. Bertini et al. (32) tested their automatic speed limit advisory system at bottlenecks along a section of German freeway, which decreased the speed limit before bottleneck activation as a means of managing traffic density.

Another notable effort in the development and deployment of crash prone traffic condition detection and alert systems is currently active in Japan. Under the Advanced cruise-assist Highway System (AHS) program, two systems relevant to this research are currently in the field deployment and evaluation stage. The first one is an automated roll-over alert system. The system is comprised of several sensors providing information on individual vehicle speed, height, and weight. It estimates the probability that a vehicle might roll-over in the approaching sharp curve. If this probability is greater than a pre-defined threshold, message signs and radio signals will alert the specific driver of the danger and require the driver to slow down. This system is based on simple physical models which determine the roll-over probability and is mainly aimed to prevent large truck crashes. The second system developed under the AHS program is more relevant to the scope of this research. This automated driver alert system aims at rear-end crash prevention at roadway sections with special geometric designs and limited visibility (e.g., sharp curve). In general, the logic of the system is straightforward: if there is a queue in the predefined position or any other lane obstruction, the warning mechanism is activated and then sends alert messages to drivers.

3.3.2.3 ILCS Applications in Minnesota

As an example of the implementation of ILCS in the State of Minnesota, one project (4) involved hanging displays permanently over the traffic lanes on key segments of I-94 and I-35W. Staff members at MnDOT's Regional Transportation Management Center (RTMC) monitor the flow of traffic through closed-circuit video cameras and sensors embedded in the pavement. When an incident occurs, RTMC staff program the ILCS units to display a series of messages directing drivers away from blocked lanes. A rich crash database was created and analyzed to investigate crash related traffic events and contributing factors such as weather, individual vehicle speed and headways, etc.

Another project (51) utilized a 3D virtual reality system to help design a warning system. Traffic data was collected from a high crash zone on I-94. This project visualized and analyzed the crash data using micro-simulation methods and highlighted gaps in technology and/or knowledge that hampered existing and future research projects with similar objectives. One of the gaps identified was the fact that the two most widely used data sources, video data and GPS data, are not accurate enough for online micro-simulation purposes. The high-resolution event-based data collected from this project could help fill that gap.

Another key to implementing ILCS systems is to make sure that each message carries a clear meaning to all drivers. Researchers have been investigating the effectiveness of ILCS messages. For instance, experiments found that the diagonal arrow merge sign is the most visible ILCS display message (visible from 266 feet on average) compared to words and dynamic chevrons (47). It has also been pointed out that the ILCS signals have different impacts on drivers at different ages. The younger a driver is, the quicker a driver is to respond. The specific effectiveness of ILCS signals tested in the field in the State of Minnesota was studied by Harder and Bloomfield (47).

3.3.2.4 Concluding Remarks

Both the simulation and field studies showed positive impacts of ILCS system on the safety of freeway. Additionally, ILCS systems also improve the mobility of the freeway traffic flow by helping drivers stabilize their speed and eliminating stop-and-go movements. Another lesson learned from the literature is that different signs carrying different information will have different levels of effectiveness on different groups of drivers. Sending out information with the best results requires well designed signs and messages. Lastly, the existing ILCS systems obtain information on traffic conditions from traditional means of data collection.

3.4 DATA COLLECTION DEVICE INSTALLATION AND DATA DESCRIPTION

3.4.1 Implementation Location

Five sets of the SMART Signal Data Collection Units (DCUs) were installed on I-35W, from 44th street to 58th street. Figure 3.1 shows the implementation locations. Each DCU collects traffic data in both directions. For example, DCU 5 collects traffic data at Station 56 (Northbound direction) and Station 10 (Southbound direction). Each of the DCUs gets an assigned IP address from the MNIT in order to send data packets back to the SMART Signal data server at the RTMC in real-time.

Table 3-1 lists the locations of MnDOT controller cabinets along the freeway, network settings of the data collection units, including IP addresses, gateway, and subnet mask.

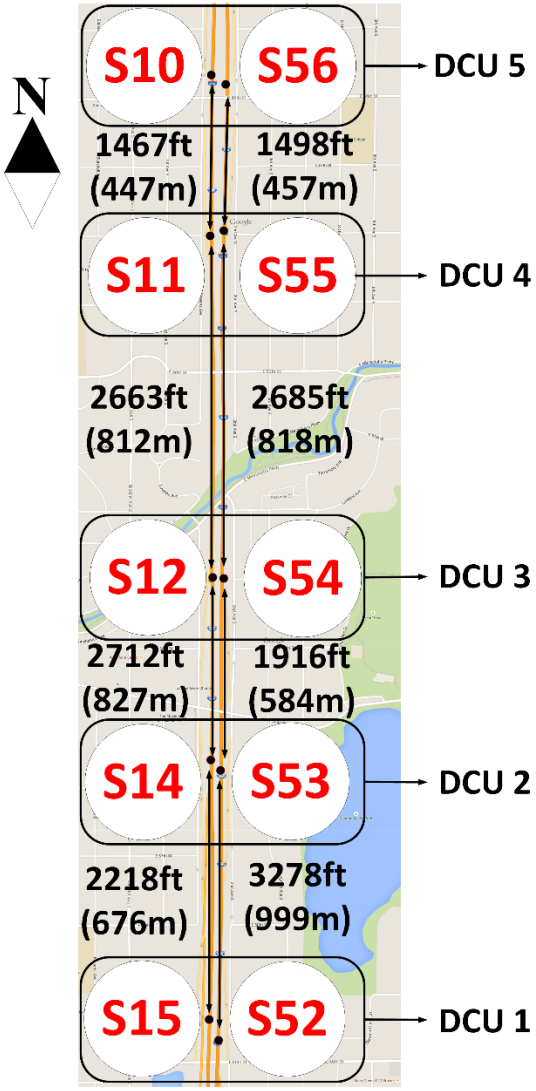

Figure 3.1 Implementation locations

Table 3-1 Implementation locations and network settings

	STATION NUMBER	CABINET LOCATION	SMART SIGNAL DCU IP ADDRESS
1	Station 52, 15	I-35W @ 58th St.	10.69.129.30
2	Station 53, 14	I-35W @ Diamond Lake Rd.	10.69.128.232
3	Station 54, 12	I-35W @ Minnehaha Pkwy.	10.69.128.222
4	Station 55, 11	I-35W @ 48th St.	10.69.128.192
5	Station 56, 10	I-35W @ 44th St.	10.69.128.162

Gateway: 10.69.128.1
Subnet Mask: 255.255.254.0

3.4.2 Detector Pin Assignment

The detectors on freeway are connected to a 170-type controller at each of the stations. The SMART-Signal DCU collects the detector actuation information through the C-1 connector of the controller via a Y-cable as seen in Figure 3.2. The device itself is plug-and-play and each station takes about 5 to 10 minutes to install.

The detector pin assignment table can be found in Table 3-2, where each of the detectors at a station is associated with a C-1 connector pin and then with a specific SMART Signal detector number. Users can refer to the table when looking at the data collected by the SMART Signal DCUs.

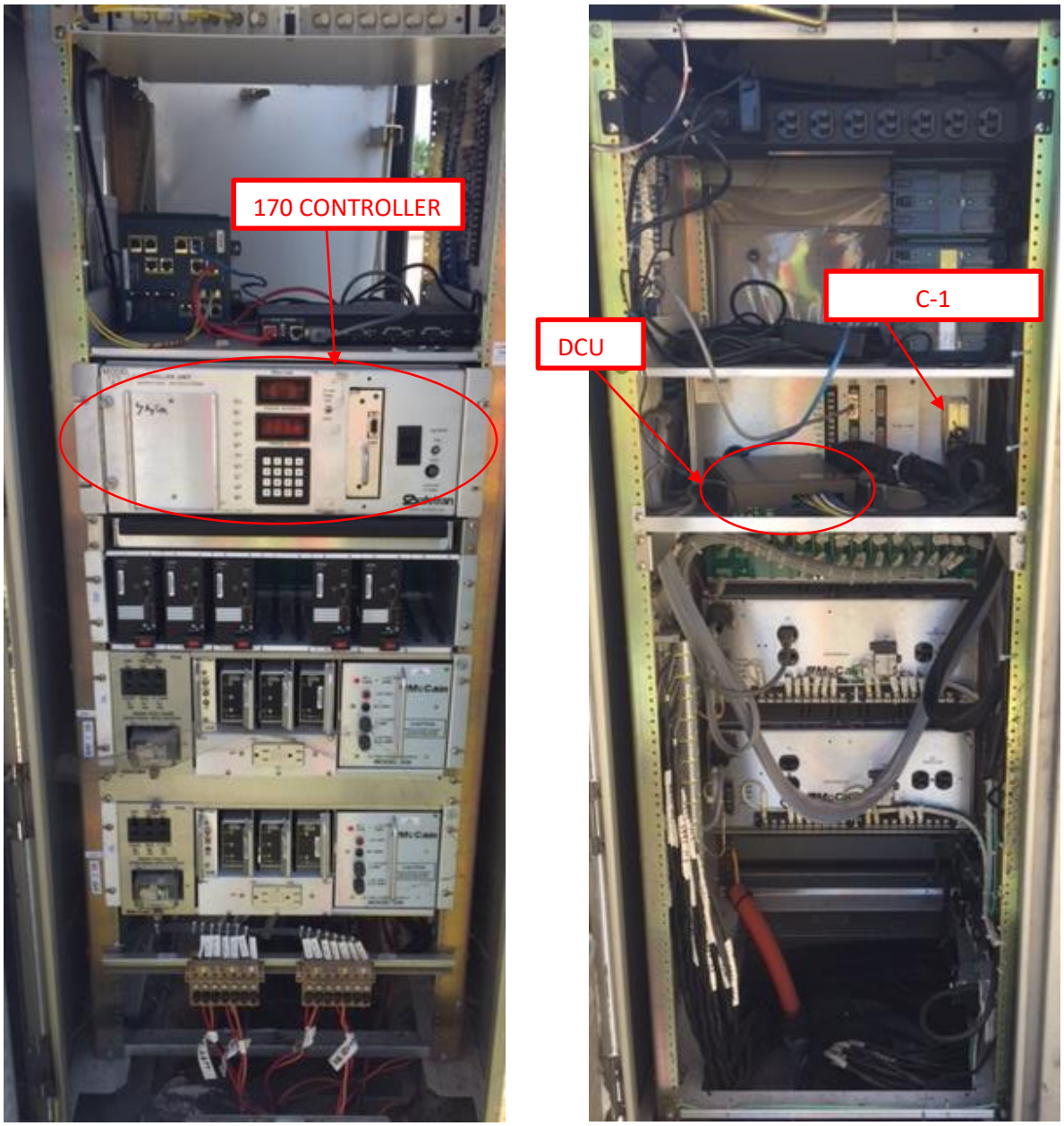

(a) (b)

Figure 3.2 Controller cabinet with data collection units

Table 3-2 Detector pin assignment table

Station Number Northbound	Detector Number	C-1 Connector Pin	SMART Signal Detector Number	Station Number Southbound	Detector Number	C-1 Connector Pin	SMART Signal Detector Number
52	300	39	1	15	222	43	5
	301	40	2		223	44	6
	302	41	3		224	45	7
	5933	42	4				
	5934	47	9				
	5935	48	10				
53	303	39	1	14	219	43	5
	304	40	2		220	44	6
	305	41	3		221	45	7
	5941	42	4		5939	46	8
	5942	47	9		5940	48	10
54	5943	39	1	12	5953	49	11
	5944	40	2		5954	50	12
	5945	41	3		5955	51	13
	5946	42	4		5956	52	14
	5947	43	5		5957	53	N/A
	5948	44	6		5958	54	N/A
	5949	45	7		5959	55	15
	5950	46	8		5960	56	16
	5951	47	9		5961	57	17
	5952	48	10		5962	58	18
55	5963	39	1	11	5972	43	5
	5964	40	2		5973	44	6
	5965	41	3		5974	45	7
	5966	42	4		5975	46	8
	5967	47	9		5976	48	10
56	312	39	1	10	207	43	5
	313	40	2		208	44	6
	314	41	3		209	45	7
	5968	42	4		5970	46	8
	5969	47	9		5971	48	10

3.4.3 Data Description

The SMART-Signal system collects and archives vehicle-detector actuation events. Each event contains the timestamp and occupancy time of one vehicle, as well as the ID of the corresponding detector. A sample of collected data is shown in Figure 3.3. For example, at 18:38:47.627 on August 5, 2015, a vehicle reached detector 9, and the time that this vehicle occupied the detector for was 0.220 seconds. The difference between the arriving times of consecutive vehicles gives the headway for these two vehicles and taking the occupancy time out of the headway gives the gap between these two vehicles. Note that each piece of event-based data is archived in the database only after the vehicle leaves the detector.

	ID	TimeStamp	DetectorID	TimeDuration
1	1018843	150805183847627	9	0.220
2	1018844	150805183847967	2	0.241
3	1018845	150805183847747	20	0.731
4	1018846	150805183847867	4	0.921
5	1018847	150805183848328	1	0.610
6	1018848	150805183848838	5	0.241

Figure 3.3 A sample of event-based data

With these high-resolution data available, macroscopic traffic flow parameters including flow rate, q, speed, v, and density, ρ, can be measured using the following equations:

$$q = \frac{1}{headway} \tag{3.1a}$$

$$v = \frac{L_e}{occupancy\ time} \tag{3.1b}$$

$$\rho = \frac{q}{v} = \frac{occupancy\ time}{L_e * headway} \tag{3.1c}$$

While occupancy is normally referred to as the percentage that a loop detector is occupied by vehicles during a fixed time period (e.g. 30 seconds or 5 minutes), for the purposes of this project occupancy refers to the time duration that a loop detector is occupied by an individual vehicle because of the use of high-resolution data.

3.5 ALGORITHM DEVELOPMENT (I-35W TEST SITE)

3.5.1 Online Queue Length Estimation Algorithm

Before going into detail, it is necessary to define the applicable scope of the online queue length estimation algorithm developed for this project. The onset of a stopped queue on freeway can occur anywhere and at any time. Due to the limited number and fixed locations of loop detectors, the occurrence time and position of the very first queued vehicle can rarely be identified. Based on the real-time data collected from detectors, the algorithm can "see" the queue only when it travels to the position of a detector. Although traffic states from detectors upstream and downstream of the queue give some information on the queue, it is risky to predict the occurrence of a queue before it reaches a detector because such prediction easily generates false alerts. Therefore, instead of capturing the exact occurrence time and location of every stopped queue, the algorithm works to monitor the queue once it is seen by detectors. For those queues starting from in-between positions and propagate to detectors, lags in response arise but the algorithm provides a more robust solution than capturing the exact occurrence time and location of every stopped queue. For those not propagating to detectors, the algorithm omits them because of their limited influence in space and time.

The algorithm runs locally in any freeway segment between two detectors, estimating the length and duration of a queue once it the queue is detected by the downstream detector. When the queue grows past the upstream detector, the algorithm stops estimating it; further estimation of the queue would be provided by the same algorithm running in the next upstream segment. Moreover, considering the difference of traffic states across lanes (e.g., lanes to different directions of a divergent junction), one algorithm runs for each lane. The algorithm also has limited capability predict the time when a queue will be formed or cleared at any given position in a segment nor can it calculate the length of the queue in the segment.

3.5.1.1 Identification of the Occurrence and Termination of Queues

The first step of the algorithm is to identify the occurrence and termination of a queue at detector locations. Generally, the occurrence of queues can be identified by checking the values of occupancy time. For example, if a vehicle has occupied the detector for ten seconds, it is safe to claim that this vehicle is stopped in a queue. However, relying solely on occupancy time may miss detection of some queues. The reason for this is that drivers may maintain following distances than detector length when stopping thereby occasionally leaving the detection area blank. In this case, vehicles are queued but no large occupancy time can be seen from the data. One example is shown in Figure 3.4. Occupancy time and headway for each vehicle are plotted. Most of the long occupancy times and long headways appear in pairs as denoted by the black circles, except for one event that is highlighted by the green circle. Note that this long headway together with very short occupancy time cannot be caused by a lack of traffic demand since it is during peak hours. Rather, this single long headway is caused by a vehicle stopped in the queue right behind the detector.

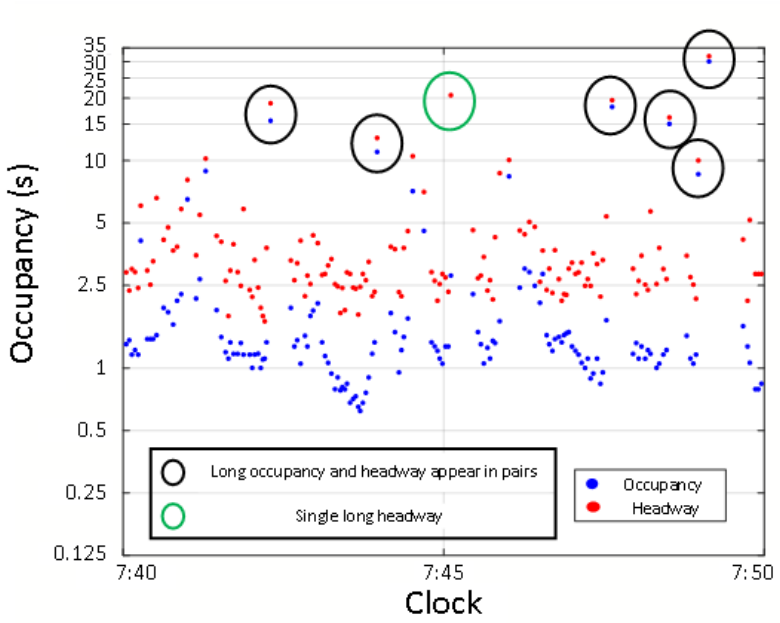

Figure 3.4 Paired and unpaired long occupancy and headway data

Another problem is that, when implementing the algorithm in the real world, the value of occupancy time is archived in the database only after the vehicle leaves the detector but, in order to estimate the queue in a timely manner, the algorithm cannot wait until the vehicle occupying the detector for an abnormally long period of time leaves the detector to begin computing. In fact, seeing a long occupancy time archived to the database usually indicates the end of the queuing state. Therefore, a combined criterion to identify the onset of queue is used as seen in Equation 3.2

$$max\big(\boldsymbol{S}(t)\big) \leq v_h \; and \; (\, G(t) \geq G_h or \; Occ > Occ_h \,) \qquad (3.2)$$

Where:

$\mathbf{S}(t)$: the set that contains the speeds of the past three vehicles,

$G(t)$: ithe time gap since last vehicle leaves the detector,

Occ: the occupancy time of the last vehicle, and v_h , G_h and Occ_h are pre-defined corresponding threshold values for them.

From Equation 3.2 it can be assumed that if the traffic becomes slow (because of a stopped queue ahead) and no new record has been seen for a long time or the most recent record has a long occupancy time, some vehicle must have stopped either at or right behind the detector location.

Identification of the termination of the queuing state is not straightforward either. When a stopped vehicle begins to move forward, it is possible that it only moves a few feet before stopping again, and so

do the following vehicles. This happens often in freeway stop-and-go scenarios when the initial queue is compressing. In this case, the move of the originally stopped vehicle does not mean the termination of the queuing state. The termination of queuing state is, instead, confirmed by satisfying the following equation

$$\min(\mathbf{S}(t)) \geq v_l \tag{3.3}$$

Where:

$\mathbf{S}(t)$: the set that contains the speeds of the past three vehicles,

v_l: another threshold value of speed.

3.5.1.2 Estimation of Queuing/Discharge Shockwave Speed

After identifying the onset and termination of queuing state, the algorithm will begin to estimate the queue by calculating the positions of its head and tail. The theoretical basis of the algorithm is shockwave theory. Shockwave takes place where two traffic states (e.g., free flow traffic state and jam traffic state) meet. The speed of the shockwave *w* can be calculated by the following equation.

$$w = \frac{q_1 - q_2}{\rho_1 - \rho_2} \tag{3.4}$$

Where:

q_1,ρ_1:flow rate and density for upstream traffic

q_2 , ρ_2: flow rate and density for downstream traffic, respectively.

Typically, there are two kinds of shockwaves in the queuing process on freeway: the queuing shockwave that is described by the position of the last queued vehicle, i.e. queue tail, and the discharge shockwave that is described by the position of the first vehicle waiting to be discharged, i.e. queue head. The traffic states near the two shockwaves are shown in the time-space diagram in Figure 3.5. From left to right, the three traffic states are arrival state, queuing state, and departure state, respectively. The boundary line between the first two states is the queuing shockwave, and the boundary line between the last two states is the discharge shockwave.

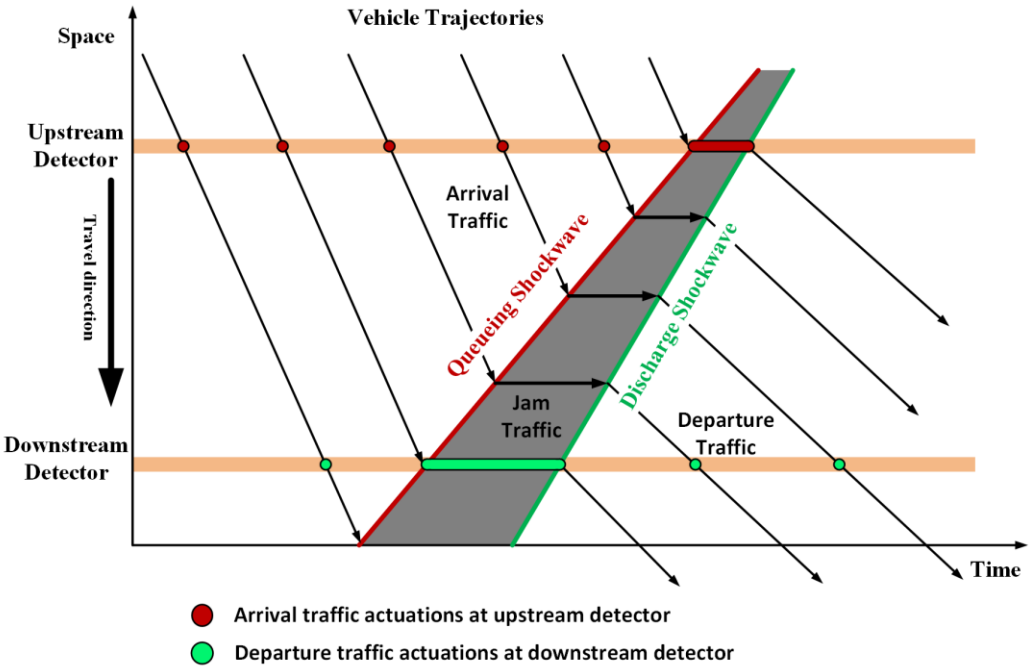

Figure 3.5 Estimation of density and flow rate

As shown in Equation 3.4, the states of arrival traffic, jam traffic, and departure traffic determine the speeds of the queuing and discharge shockwaves. The flow rate of jam traffic is zero, and a constant jam density can be assumed and calibrated using historical data. Therefore, the key problem is to estimate the arrival traffic state and departure traffic state. Once a jam is detected at the downstream detector, the data collected from the upstream detector for several preceding vehicle actuations are put into Equation 3.1 to estimate the density and flow rate of the arrival traffic and calculate queuing shockwave speed (see Figure 3.5). The following several vehicle's detector-actuation data from the upstream detector will be utilized to update the arrival traffic state and the speed of the queuing shockwave as long as the traffic state at the upstream detector does not stabilize. In the algorithm, updates to the queuing shockwave speed will be ended if the variance of speed and flow rate of consecutive vehicles from the upstream detector are very small. The speed of the discharge shockwave is estimated in a similar way. Vehicle actuations at the downstream detector after the termination of the queuing state will be used to initialize and update the speed of the discharge shockwave. Again, the update will be ended when the traffic state at the downstream detector stabilizes.

3.5.1.3 Estimation of Queue Position

With the speeds of the two shockwaves, the positions of the queue tail and queue head can be easily derived. Denoted respectively by $d_l(t)$ and $d_h(t)$ the distances from the positions of queue tail and queue head to the position of downstream detector at time t. It is worth noting that the initial value of either $d_l(t)$ or $d_h(t)$ is not zero because of the time lag in identification of the onset or termination of queuing state as discussed in Section 3.5.1.1. Their initial values are derived by multiplying the initial

shockwave speed by a time delay. Afterwards, the positions of the queue tail and queue head will be calculated step by step. Let τ denote time interval of each time step, $d_l(t)$ and $d_h(t)$ can be calculated by the following equations:

$$\begin{aligned} d_l(t+\tau) &= d_l(t) + w_q(t) \times \tau \\ d_h(t+\tau) &= d_h(t) + w_d(t) \times \tau \end{aligned} \tag{3.5}$$

where $w_q(t)$ and $w_d(t)$ are the speeds of queuing and discharge shockwaves at time t, respectively.

Following that, the length of the queue at any time, $q_l(t)$, and the duration of the queue at any space, $q_t(x)$, can be easily derived as follows:

$$\begin{aligned} q_l(t) &= d_l(t) - d_h(t) \\ q_t(x) &= t_2 - t_1, where\ d_l(t_1) = d_h(t_2) = x \end{aligned} \tag{3.6}$$

As mentioned before, the algorithm will not update shockwave positions beyond the position of the upstream detector. Moreover, if the discharge shockwave catches up to the queuing shockwave, meaning that the queue in the segment has been cleared, the current queuing and discharge shockwaves will be cleared and the update will be stopped, too.

A flowchart of the queue estimation algorithm is shown in Figure 3.6. This algorithm updates all of the information (downstream traffic state, queue head, queue tail, shockwave speed, etc.) at every time step in real time.

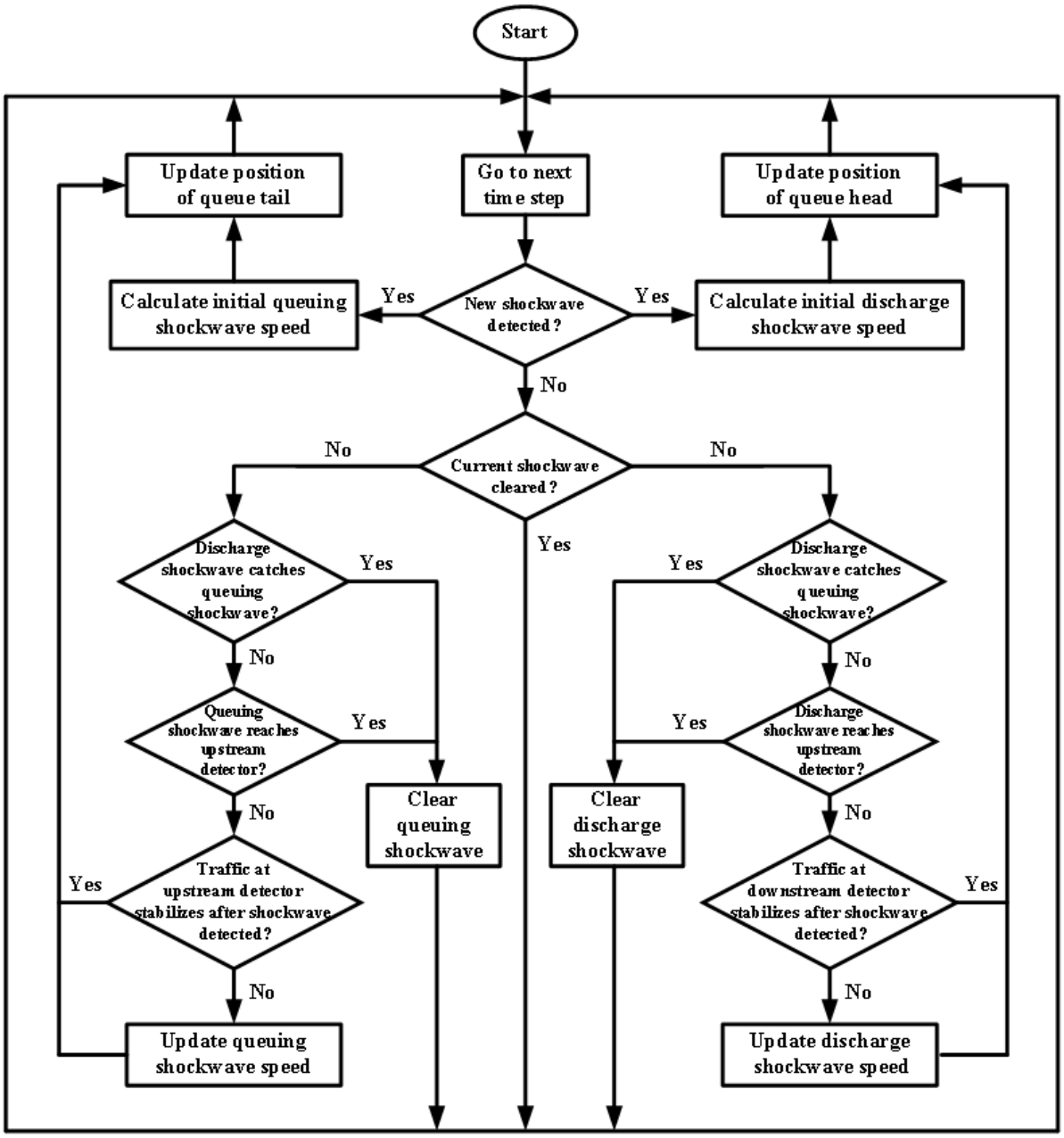

Figure 3.6 Flowchart of the queue estimation algorithm

3.5.1.4 Impact of Lane Change on Shockwave Speed

One assumption of the shockwave model is that vehicles do not change lanes when traversing the subject segment. This assumption generally holds true for queues on urban arterials near intersections because vehicles are not permitted to change lanes. However, for most freeway segments, vehicles can change lanes as long as they do not impede others. Vehicles passing the upstream detector may change lanes before joining the queue in the subject lane, and vehicles departing from the queue in the subject

lane may change lanes before showing up at the downstream detector. In this case, using data only from upstream and downstream detectors in the subject lane to estimate queue may cause non-negligible errors. To address this problem, a well-recognized lane change model, i.e., the gap acceptance model, is adopted to modify the original algorithm. Generally, lane changes are executed when drivers are motivated to do so and safe gaps in both lanes exist. To this end, the traffic states of adjacent lanes are considered as well. For example, if the subject lane is very congested while the adjacent lanes have less traffic and safe gaps, drivers from the subject lanes will be motivated to change lanes to avoid congestion. In the modified algorithm, the differences in the density and speed across lanes are checked and the number of available gaps that exceed a thresholdsize are counted. Using the information on density and speed differences and the number of available gaps, the percentage of vehicles changing lanes can be estimated and used to modify the queuing shockwave speed using the following equation

$$w_q{}'(t) = w_q(t) \times (1 - \frac{n}{N})$$
$$w_d{}'(t) = w_d(t) \times (1 + \frac{n}{N}) \quad (3.7)$$

where n is the number of gaps exceed the threshold, and N is the number of sampled vehicles.

3.5.1.5 Traffic State Merging for Queuing and Slow-moving States

Unlike the queuing process on urban arterials near intersections, it is sometimes difficult to distinguish one jam from another on freeway segments. As mentioned before, traffic state changes on freeways do not have fixed periods or modes. The traffic state can change from stopped queuing to slow-moving and then quickly go back to the stopped queuing state again. Therefore, it is necessary to merge two or more consecutive traffic jams into one. This modification is also important in practice because many active traffic management (ATM) strategies (e.g., warning of stopped traffic) seek to avoid changing traffic information too frequently.

One example is shown in Figure 3.7(a) shows the case without merge. The times of the start and end of the first jam are identified as times t_1 and t_2, respectively. The times of the start and end of the second jam are identified as times t_3 and t_4, respectively. Note that when the second jam is detected at the downstream detector, the previous jam has not reached the upstream detector. This jam-slow-jam traffic is likely to become a large jam upstream. In this case, the downstream traffic state between t_2 and t_3 is checked. If the average speed is below a certain threshold v_m, then it will be re-categorized as jam traffic. This jam-slow-jam traffic is combined into a large jam, as shown in Figure 3.7(b).

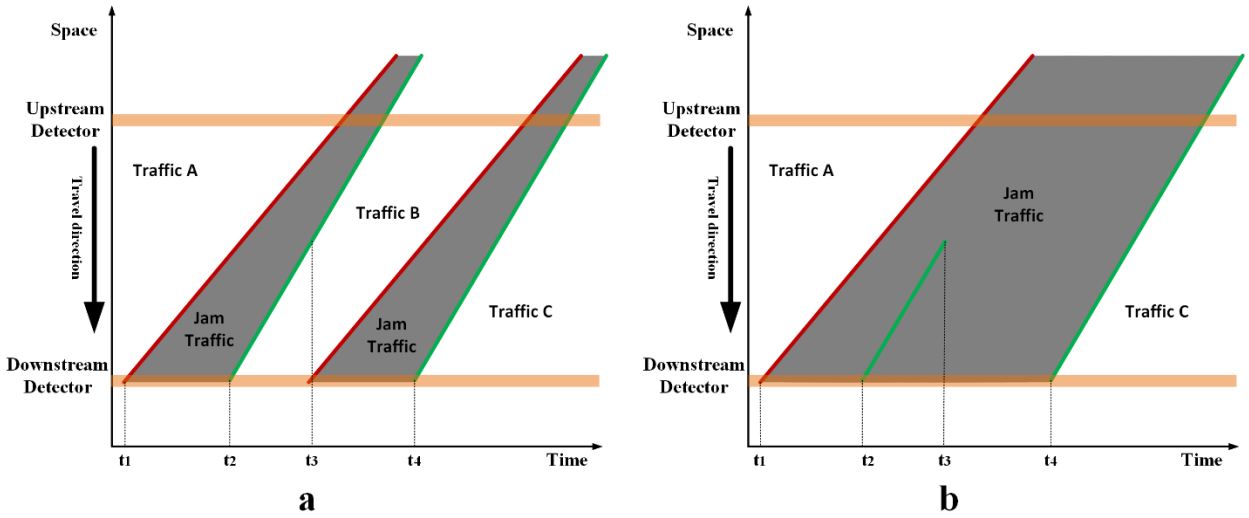

Figure 3.7 Merge of jam traffic: (a) without merge; (b) with merge

3.5.1.6 Prediction Ability

The ability to predict future traffic states is essential to any queue estimation algorithm. It can help ATM methods to react in a timely manner. The prediction ability of a queue estimation algorithm is measured by how early a reliable prediction can be made relative to the time that the real traffic state changes at the position of interest. In the proposed queue estimation algorithm, although shockwave speed can be continuously updated after it takes place, it has been found that the speed will converge to a certain value after five to ten updates. Then a constant shockwave speed can be set and the position of the head or tail of queue in the near future predicted. The prediction ability of the algorithm depends on the distance from the location of interest to the downstream detector, the shockwave speed, and the time needed before the traffic stabilizes.

$$T_p = max\left\{\frac{x - d_h(t_s)}{w}, 0\right\} \tag{3.8}$$

where T_p is the prediction ability, x is the distance from location of interest to downstream detector, t_s is the interval from begin of discharge to the time when the traffic stabilizes, and w is the stabilized shockwave speed.

Note that the prediction ability of the proposed algorithm is limited; predictions cannot be made for locations near the downstream detector.

3.5.2 Field Test of Queue Estimation Algorithm

The proposed algorithm is tested with field data. The data were collected on a 2218-foot-long segment of I-35W between detector stations S14 and S15. The layout of the loop detectors on I-35W for the

southbound direction is shown in Figure 3.8. In this segment, traffic on I-35W goes southbound and merges onto I-35W or TH62 at the junction. There are five lanes (L1-5 from west to east in Figure 3.8) at the north end of the segment and three lanes for each branch after diverging, including a high-occupancy toll (HOT) lane in the east most lane. In the morning peak, vehicle queues often propagate from downstream of the I-35W branch. L4 is the most congested lane during this period so Detector 6 at Station S15 (D6-S15) and Detector 8 at Station S14 (D8-S14) were selected as the downstream and upstream detectors, respectively. L3 is less congested because some traffic merges off of I-35W and onto TH62 at the junction so D5-S15 and D7-S14 were used as the adjacent detectors. Although L5 has even less traffic, it was not considered as an adjacent lane of L4 because vehicles rarely make lane changes into or out of a HOT lane. We set the following parameters: $L_e = 27$ ft, $v_h = 45$ mph, $G_h = 9$ s, $Occ_h = 3.5$ s, $v_l = 9$ mph, $\rho_{jam} = 180$ veh/mi, $q_{jam} = 0$ veh/h, $\tau = 1$ s, $v_m = 23$ mph. According to the proposed queue estimation algorithm, the positions of the two shockwaves can be calculated by Equation 3.5. The spatial length of a queue at any time and the temporal duration of a queue at any position in between S15 and S14 can be calculated by Equation 3.6. For the sake of verification, predicting the duration of the queue at S14 is the focus of the test due to the availability of ground truth data.

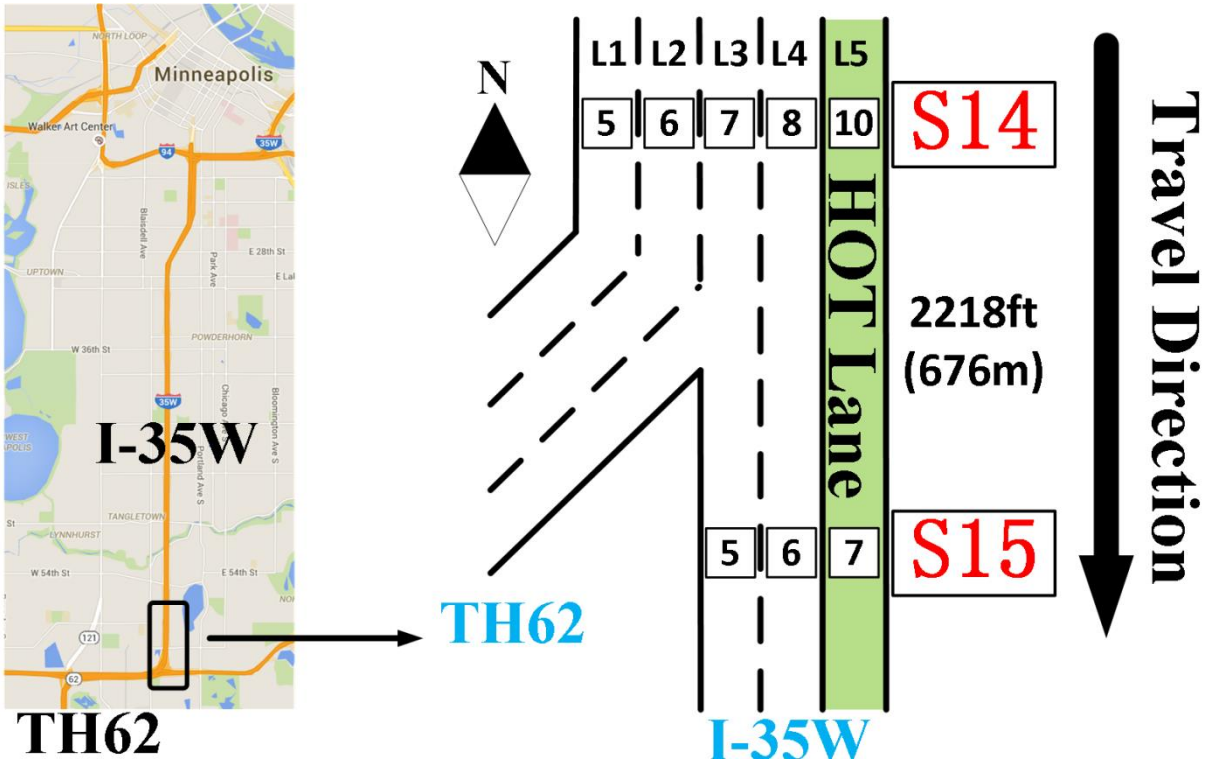

Figure 3.8 Layout of loop detectors on a southbound I-35W segment

One busy morning peak on August 5, 2015, is selected to evaluate the performance of our algorithm. Traffic states at upstream detector D8-S14 were estimated by a series of queuing and discharge shockwaves, as shown in Figure 3.9. At any time, if an estimated queuing shockwave has arrived at the upstream detector and no discharge shockwave has arrived afterward, the traffic state at that time is

estimated as a jam state; otherwise, it is estimated as a non-jam state. The ground truth is shown in Figure 3.9 by depicting every individual vehicle-detector actuation event at the positions of both upstream detector D8-S14 and downstream detector D6-S15. Each event is depicted as a bar with the length of its occupancy time. The color of the bar indicates different traffic states.

During the studied period, nine queues were estimated from the proposed algorithm, as shown in Figure 3.9. The unfinished green lines are intentionally left to show the merge of jam-slow-jam traffic as discussed in the previous section. On inspection, it can be seen that the estimated queues in green and red encompassed all of the stopped traffic (black bars) at the upstream detector, indicating that the queuing states at upstream were effectively estimated by the proposed algorithm. Figure 3.9 also shows the necessity of merging short jams. Without merging, there are roughly 37 queues at the upstream detector. With merging, the number is reduced to 9.

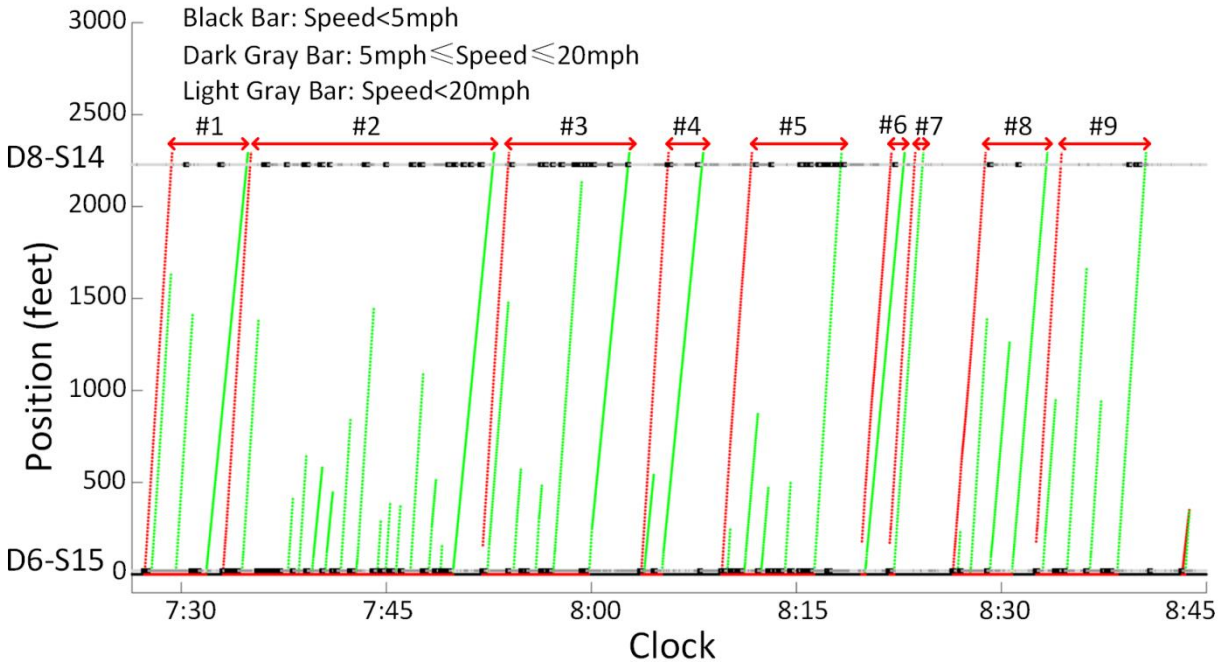

Figure 3.9 Queue estimation results

To quantitatively evaluate the algorithm, the average speed, flow rate and density were chosen as the measures of effectiveness (MOEs). The MOEs of the nine estimated jam states and their adjacent non-jam states were calculated using high-resolution data from D8-S14, as shown in Figure 3.10 (a)-(c). Ideally, the average speed and flow rate of each jam state would be significantly lower than those of its adjacent non-jam states and the average density should be significantly higher than those of its adjacent non-jam states. In this test, however, the estimated jam states at D8-S14 are not as congested as those at D6-S15 because vehicles are often able to change to the less congested lane L3. Also, note that the jam state at D8-S14 contains not only stopped traffic but also slow traffic after the merge. Despite all of these confounding factors, most of the estimated jam states can be verified by the ground truth data, especially for long queues #2, #3 and #5. The estimation of queue #6 is worth noting; Figure 3.9 shows

that there is no single vehicle-actuation event that has a long occupancy time (i.e., black bar) at D6-S15. Rather, the onset of the queuing state was identified by noting a long gap between two consecutive events, as discussed in Section 3.5.1.1. By doing this, the jam state at D8-S14 was successfully estimated by queue #6. No queues were undetected in the test, but there was one false alarm. Queue #7 is triggered by one single long occupancy event at D6-S15, but this queue did not propagate to the upstream as estimated. One possible reason for the miscalculation is the heterogeneity of human drivers. Conservative drivers may slow down their vehicles long before they join the queue. In this way they can avoid fully stops on freeway, thus smoothen the traffic. Lastly, the prediction ability is shown in Figure 3.10 (d). On average, the algorithm can predict traffic state changes at the upstream detector more than 90 seconds before the change actually occurs. Discharge states can usually be predicted earlier because the speed of the discharge shockwave is lower than that of the queuing shockwave.

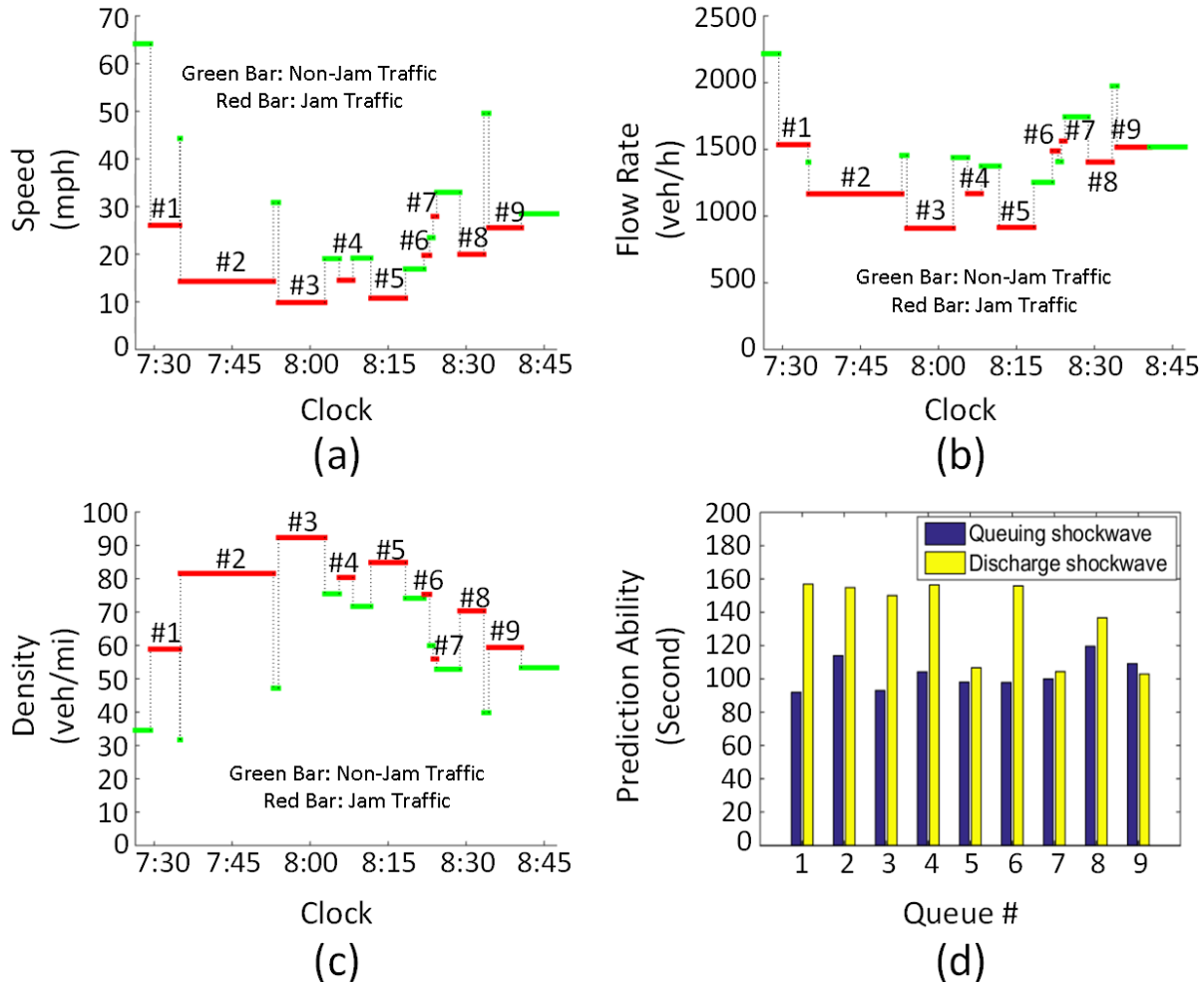

Figure 3.10 MOEs of the field test: (a) speed; (b) flow rate; (c) density; (d) prediction ability

In this field test, stopped traffic is defined by the presence of vehicles with speed lower than 5 mph. In practice, the definition of stopped traffic should be predefined by traffic operators and then the thresholds such as G_h, Occ_h, v_h and v_l should be carefully chosen. For example, it can be expected that

the larger G_h and Occ_h are, the fewer queues the algorithm estimates thereby resulting in more undetected queues but fewer false alarms.

3.5.3 Algorithm of Triggering Queue Warning Messages

Triggering queue warning messages is based on the real-time estimation of queue length. Note again that both the queue estimation algorithm and message triggers are lane-based. Once a stopped queue begins and propagates a certain distance, the queue warning message will be shown on the VMS of that lane. The distance threshold value should be large enough to confirm the queuing state and avoid false alarms, but not so large as to delay the message for too long. The distance threshold value was selected to be 1000 feet by trial-and-error. Once the queue is cleared at the downstream detector or has already reached the location near the VMS, the warning messages are no longer displayed. The communication delay between the queue warning system and message activation system should be considered as well. The algorithm was tested by RTMC engineers before its implementation and validated by checking field videos with the help of the MTO.

3.6 SYSTEM DEPLOYMENT AND EVALUATION

With the queue estimation algorithm described in Chapter 4, a queue warning system was developed for the I-35W site. With help from MnDOT engineers the message “SLOW TRAFFIC AHEAD” was selected, and the system was tested for 6 weeks (including 3 weeks testing without showing messages). The dynamic queue warning system was deployed on September 27, 2016. Figure 3.11 shows that the queue warning system was displaying a warning message specifically to the third lane from the left.

Figure 3.11 The queue warning system displaying warning message

3.6.1 Queue Warning System Development

The queue warning system for the I-35W site is shown in Figure 3.12. Real-time high-resolution vehicle actuation data were collected from three detector stations, namely S12, S14 and S15, and archived in the SMART-Signal server database. The queue warning software was developed to retrieve these data, estimate the queue length every second based on the algorithm proposed in Section 3.5.1, and then decide when and where to show the message of "SLOW TRAFFIC AHEAD". The messages were read by the Intelligent Roadway Information System (IRIS) from MnDOT and then displayed on the corresponding VMS located upstream of S12.

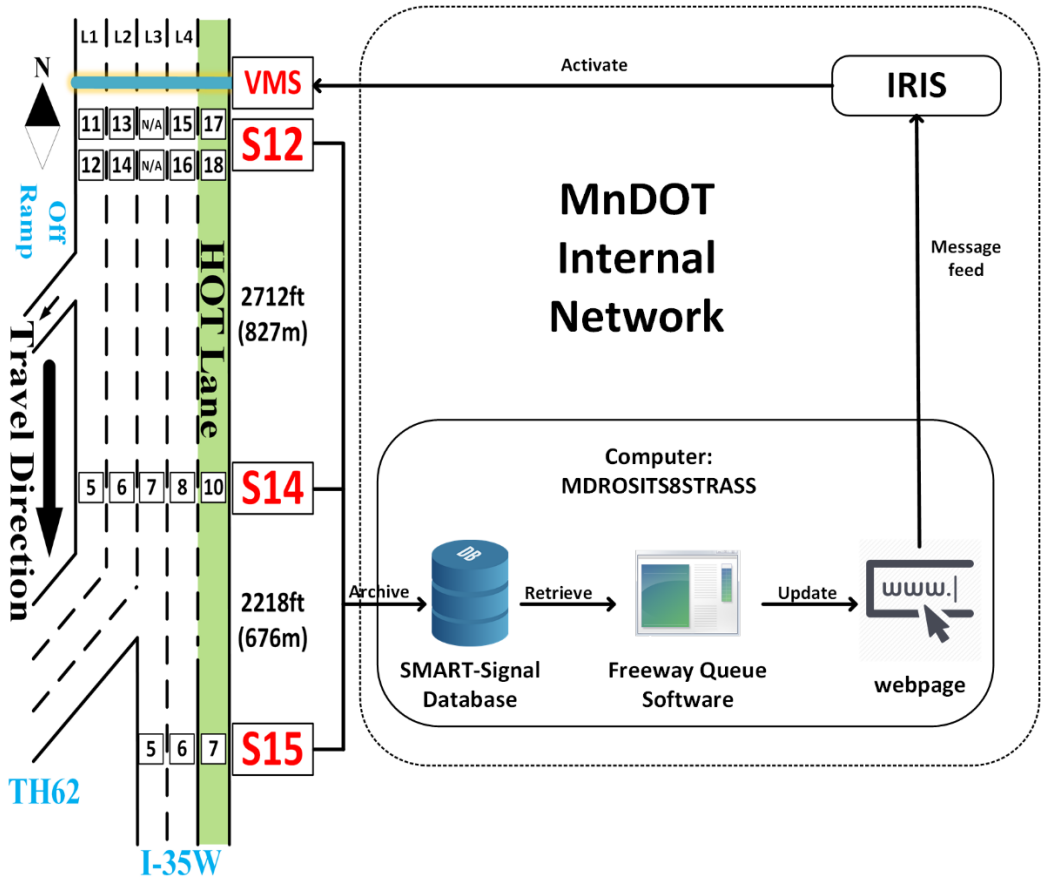

Figure 3.12 System structure

Note that the queue estimation and decision to show the warning messages are done on a lane-by-lane basis. Generally, the traffic states of each lane (except HOT lane) are monitored separately at downstream detector stations S14 and S15. If a stopped queue is detected and the estimated queue length exceeds a certain threshold on any lane, the warning message will be activated on the VMS of that lane. Considering the fact that vehicles in some lanes may change lanes together (e.g., Lane 1 and Lane 2 to the direction of TH62), warning messages on these lanes are shown together if the queue length is long enough on any of the lanes. Once the downstream queue is discharged, the warning

messages will be turned off. If queues spill back to S12, the system will also stop giving the warning message on the corresponding lane so as to avoid confusing drivers that have already joined the queue.

A snapshot of the software is shown in Figure 3.13. The upper middle pane of the software interface shows the current time. A static map of the place of interest is shown in the middle pane. The middle left and middle right panes show real-time traffic information including the timestamp, occupancy time, headway, gap, and speed of each vehicle passing by the corresponding detector station. The lower left and lower right panes show the estimated queue length when under queuing conditions. There are four black boards (VMS) on the upper part of the software with each one corresponding to one lane (HOT lane is not included). The left two VMSs (Lane 1 and Lane 2) correspond to the left lanes that merge onto TH62 direction. The rightmost VMS (Lane 4) corresponds to the lane that goes to I-35W direction. The VMS on Lane 3 corresponds to the middle lane that can either exit onto TH62 or stay on I-35W.

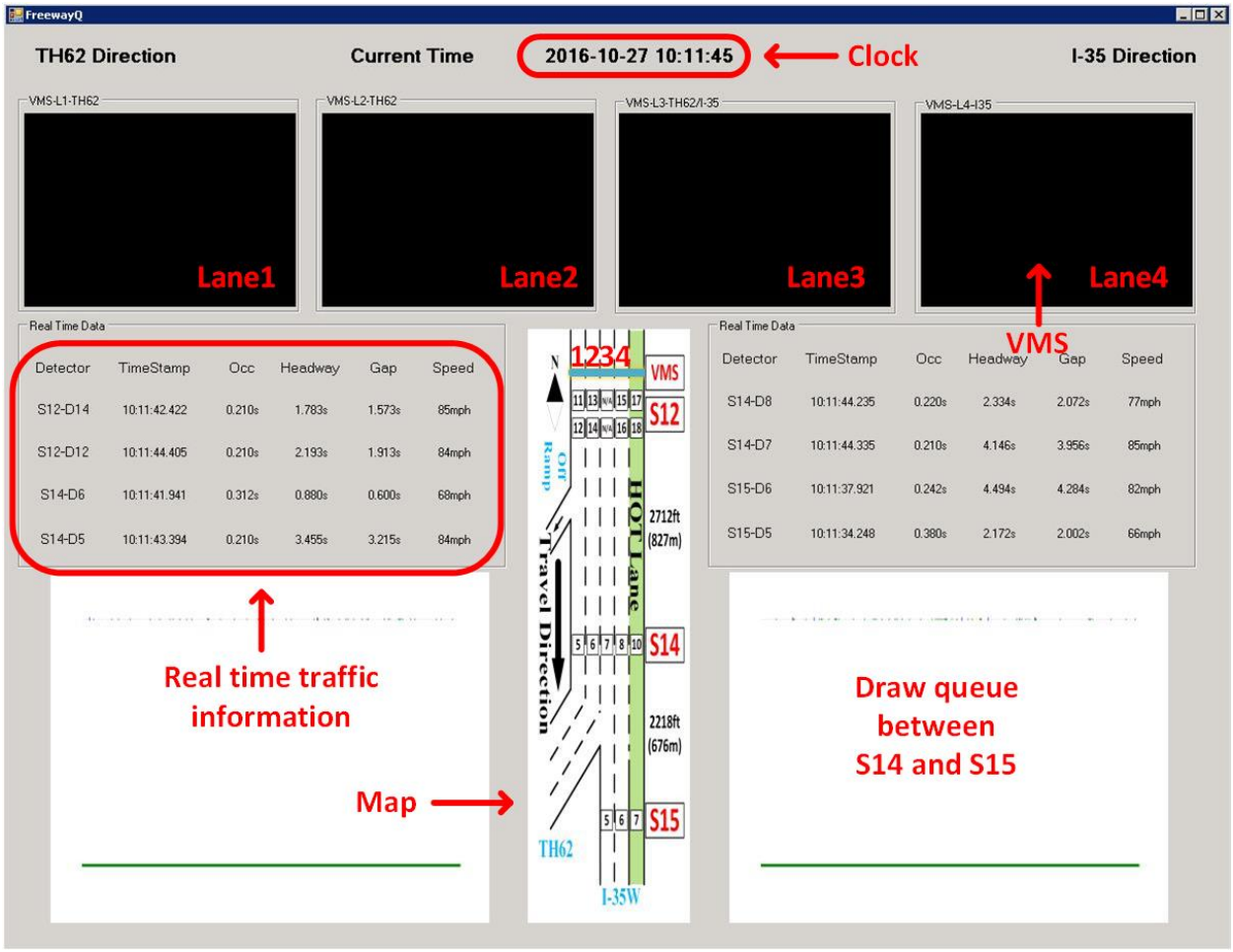

Figure 3.13 A snapshot of the developed software

To facilitate the trial run of the queue warning system as well as to ensure safety, all the data flow are within the internal network of MnDOT. The software is running on a MnDOT computer (name of the computer: MDROSITS8STRASS; IP address: 10.69.3.29), which also serves as the server of the SMART-

Signal system that archives high-resolution traffic data in real time. In MnDOT, the VMS is activated by IRIS at the request of an external system by using the "msg feed" protocol. Once the developed software decides to put a message on VMS, it will write the message to a text file. This text file can be reached at http://10.69.3.29/msgfeed/test.txt within MnDOT's internal network. IRIS polls this HTTP URL every 30 seconds and updates the VMSs accordingly.

3.6.1.1 Evaluation of Warning Messages

Following the advice of MnDOT, this task evaluates the warning message of "SLOW TRAFFIC AHEAD". The data collected for evaluation are mainly from loop detectors. Video data are also used to check the effectiveness of the system. To compare the results, 3 weeks' data before the deployment (from September 6 to September 26, 2016) and 3 weeks' data after the deployment (from September 28 to October 18, 2016) were used. A total of 1,176 warning messages were triggered by the queue warning system for the before case. Note again that those warning messages were not really shown on VMS. A total of 999 warning messages were triggered by the queue warning system for the after case. Those warning messages were shown on the VMS. For each message, the period of interest is the period when the message is turned on plus one minute after the message is turned off. The one-minute post-message period is also considered because the effect of warning messages extends beyond the time of deactivation.

3.6.1.2 Hypothesis Testing for Changes Before/After Deployment

Based on the before and after data collected, the mean value and standard deviation of speed were calculated for each detector and for each message and hypothesis testing was then carried out to see whether there was significant change before and after the deployment of the system (note that consecutive messages are combined into one single message in this part). Take the mean speed at detector station S14 (see Figures 3-15 and 3-16) as an example.

In order to confirm whether the mean speed after deployment is statistically significantly lower than that before deployment, the following hypothesis test is performed:

Two-sample hypotheses concerning the means:

$X_{1i} = \text{average speed during } i\text{th message, before the deployment;}$

$n_1 = \text{number of separate messages, before the deployment (consecutive messages are combined);}$

$X_{2j} = \text{average speed during } j\text{th message, after the deployment;}$

$n_2 = \text{number of separate messages, after the deployment;}$

$\alpha = 0.05;$

Assume $X_{1i} \sim N(\mu_1, {\sigma_1}^2)$, $X_{2j} \sim N(\mu_2, {\sigma_2}^2)$

H_0: $\mu_1 \geq \mu_2$, i.e. mean speed does not increase after the deployment.

H_1: $\mu_1 < \mu_2$, i.e. mean speed increases after the deployment.

Rejection region: $t_{v1+v2} \leq t_{v1+v2}(\alpha)$;

$v_1 = n_1 - 1; \bar{X}_1 = \frac{1}{n_1}\sum_{i=1}^{n_1} X_{1i}; s_1^2 = \frac{1}{n_1 - 1}\sum_{i=1}^{n_1}(X_{1i} - \bar{X}_1)^2;$

$v_2 = n_2 - 1; \bar{X}_2 = \frac{1}{n_2}\sum_{j=1}^{n_2} X_{2j}; s_2^2 = \frac{1}{n_2 - 1}\sum_{j=1}^{n_2}(X_{2j} - \bar{X}_2)^2;$

$S_p^2 = \sqrt{\frac{(n_1-1)s_1^2 + (n_2-1)s_2^2}{n_1+n_2-2}};$

$$t_{v1+v2} = \frac{\bar{X}_1 - \bar{X}_2}{\sqrt{\frac{S_p^2}{n_1} + \frac{S_p^2}{n_2}}}.$$

The results are shown in the Table 3-3.

Table 3-3 Hypothesis test (test hypothesis that mean speed at S14 remains the same)

	n_1	n_2	t_{v1+v2}	$t_{v1+v2}(\alpha)$	Conclusion	p-value
S14 – Lane 1	160	142	2.6768	-1.6499	Accept H_0	0.9961
S14 – Lane 2	160	142	0.1257	-1.6499	Accept H_0	0.5500
S14 – Lane 3	217	181	-2.1832	-1.6487	Reject H_0	0.0148
S14 – Lane 4	59	60	0.6246	-1.6580	Accept H_0	0.7333

With a confidence level of α = 0.05, it is concluded that the null hypothesis (H_0) that the mean speed on Lane 3 at S14 does not increase after the deployment should be rejected. Therefore, the speed on Lane 3 at S14 after the deployment is significantly higher than that before deployment. For other lanes, there is no evidence that the speed increases.

3.6.1.3 Speed Changes at S12 Before/After Deployment

The mean value and standard deviation for speed at three lanes of detector station S12 are shown in Figure 3.14. Note that detector data on Lane 3 at S12 are not available. Overall, the speed did not change much before and after the deployment of the system. The mean speeds for Lanes 1, 2, and 4 shown in Figure 3-14 The hypothesis testing did not show any statistically significant change between the before values and the after values. The main reason for this lack of variation is the fact that detector station S12 is very close to the position of VMS where drivers may not have enough time to take any action after seeing the messages.

3.6.1.4 Speed Changes at S14 Before/After Deployment

The mean value and standard deviation for speed at three lanes of detector station S14 are shown in Figure 3.15. The hypothesis testing showed with 95% confidence level (α=0.05), that after the deployment of the system, the mean speed on Lane 1 at S14 decreased, the mean speed on Lane 3 at S14 increased, the standard deviation of speed on Lane 1 and Lane 4 at S14 decreased, and the standard deviation of speed on Lane 3 at S14 increased.

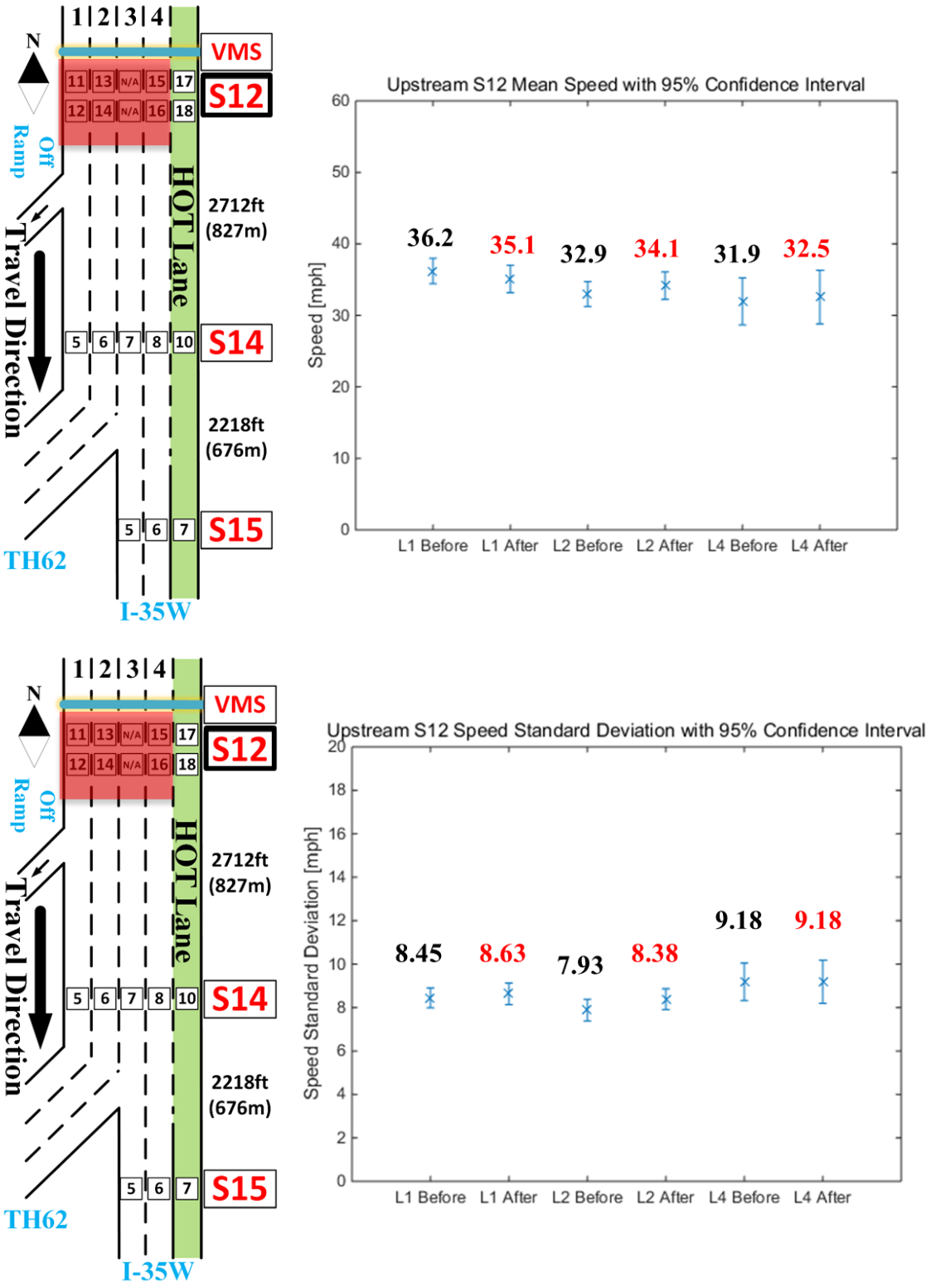

Figure 3.14 Mean value and standard deviation of speed at S12

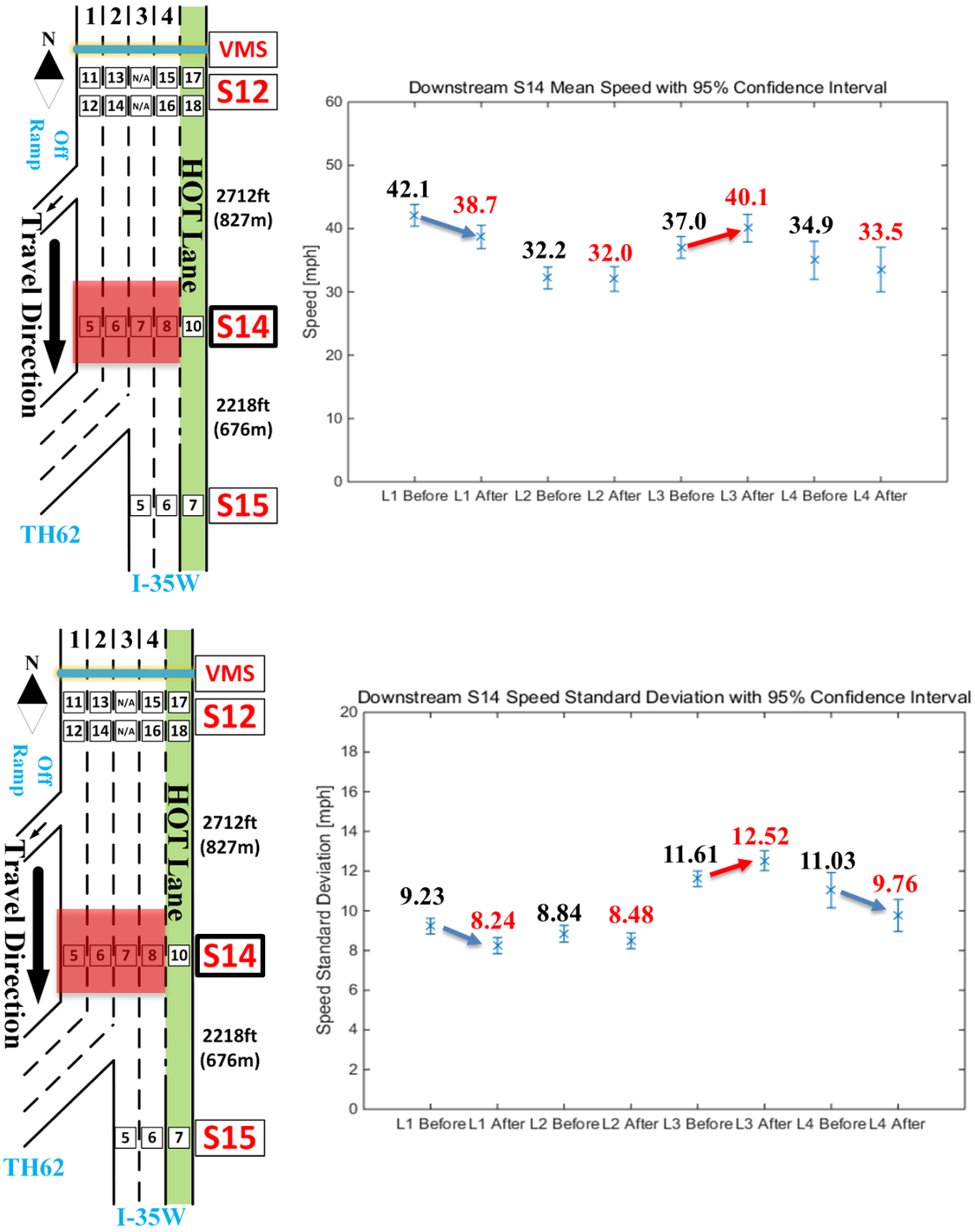

Figure 3.15 Mean value and standard deviation of speed at S14

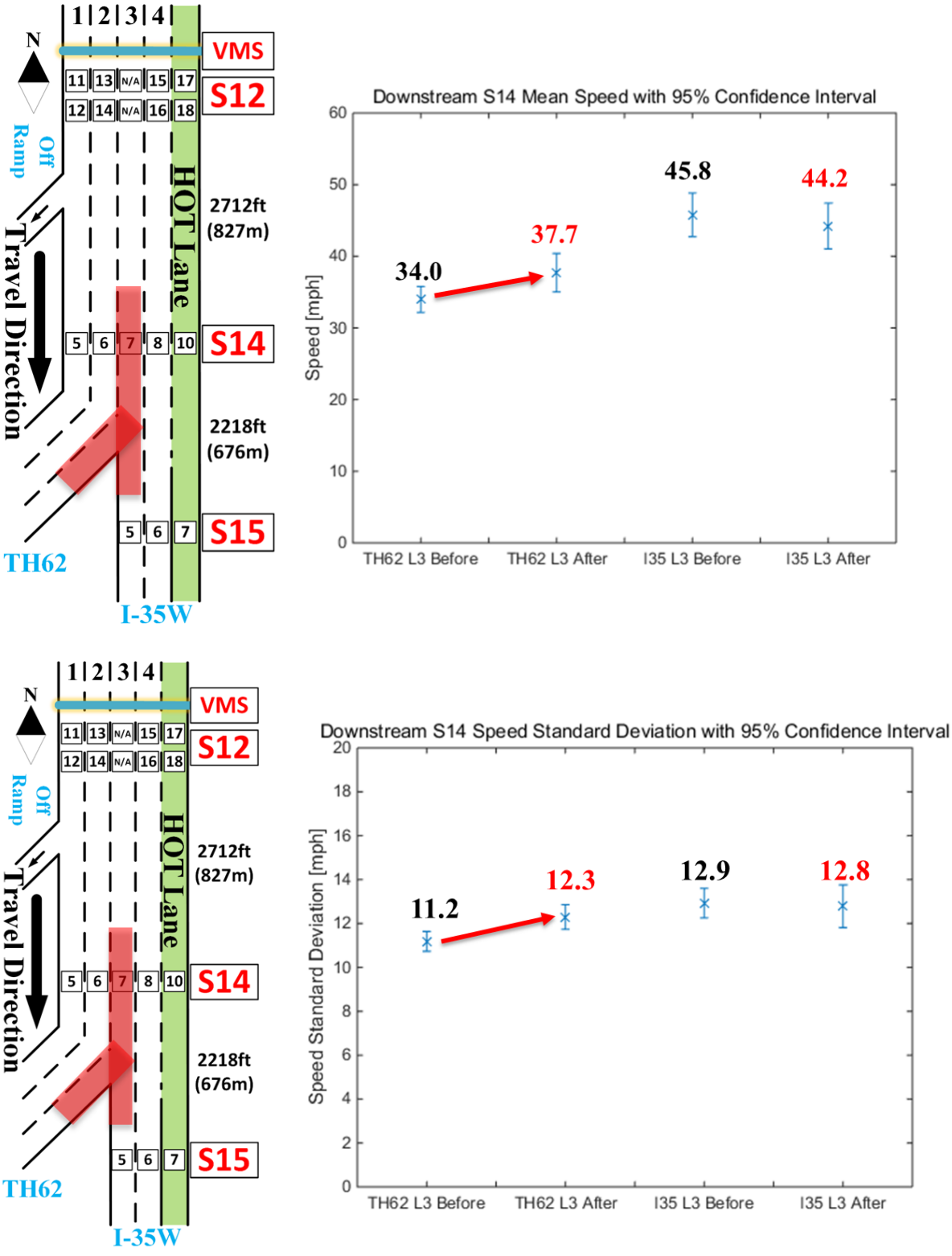

Figure 3.16 Mean value and standard deviation of speed on Lane 3 at S14: TH62 direction and I-35W direction

It is expected that the queue warning system can help smooth traffic and, in the case of traffic queues building up from downstream locations, it is hoped that drivers can decelerate in advance after seeing the warning messages shown on upstream VMS to avoid dangerous situations. To this end, the decreased standard deviation of speed in Lane 1 and Lane 4 at S14 after the deployment of the system showed positive effects. However, the standard deviation of speed at Lane 3 at S14 increased after deployment. To find the reason for this counter-intuitive result, further analysis was conducted and is contained in the following sections.

3.6.1.5 Speed Changes at the Diverging Location: Lane 3 at S14

Note that the counter-intuitive result came from Lane 3 at S14, which has two diverging lanes toward downstream locations. Vehicles on Lane 3 at S14 can go to either I-35W direction or TH62 direction. Also, vehicle queues can originate from either I-35W or TH62 and propagate back to Lane 3 at S14. Therefore, the warning messages on Lane 3 were further divided into two groups by queue source. As shown in Figure 3.16, it was found that when the queue came from I-35W, the mean value and standard deviation of speed on Lane 3 at S14 did not change much but when the queue is from TH62, the mean value and standard deviation of speed on Lane 3 at S14 increased.

3.6.1.6 Speed at Further Downstream in TH62 direction

To find the reason for the increase of the standard deviation of speed in Lane 3 at S15, especially when the messages are triggered by queues from TH62, the speed was checked at detectors further downstream, namely S1718 on TH62. Because high-resolution data at S1718 was not available, the data extraction found on MnDOT's website was utilized to get the mean speed for every 30-second interval, as shown in Figure 3.17. The mean speeds were significantly different in different lanes at S1718 because these three lanes go to different downstream directions of TH62 (eastbound and westbound). More importantly, the mean speeds in Lane 3 at S1718 were extremely low (7.2 mph and 7.3 mph), indicating that the downstream eastbound direction of TH62 was badly congested. In other words, the queues on Lane 3 at S1718 were not cleared during the studied period, and thus had a great impact on the traffic on Lane 3 at S14. This may account for the difference in results between Lane 3 at S14 and the other lanes.

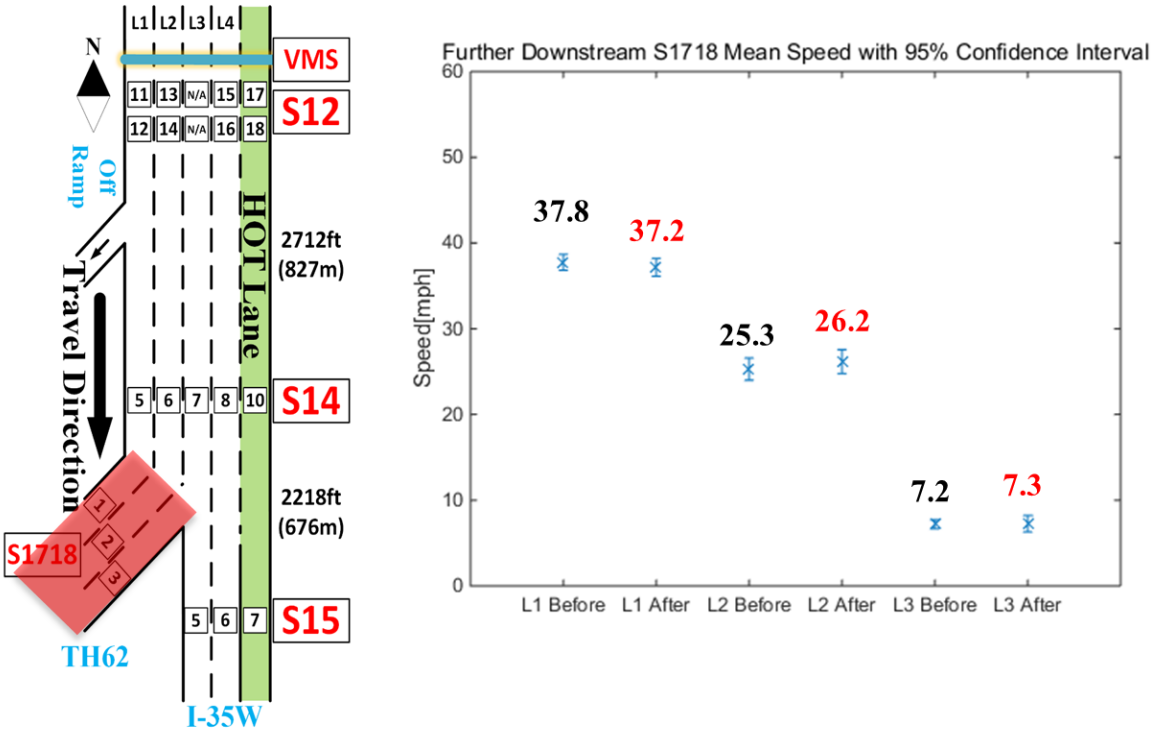

Figure 3.17 Mean speed at S15: further downstream in I-35W direction

3.6.1.7 Speed Difference across Detector Stations

The following component of the evaluation checks whether queue warning messages help decrease the speed difference across detector stations. Two pairs of consecutive detector stations were studied, namely, S12 and S14 and S14 and S1718. The mean values of the speed differences between Stations S12 and S14 were more concentrated around 0 after the deployment. If ±5 mph was chosen as the satisfactory speed difference range, almost all of the pairs had speed differences within this range after deployment (Figure 3.18). For S14 and S1718 in TH62 direction, the speed difference in Lane 3 remained roughly constant at a large value but the speed differences in Lane 1 and Lane 2 were significantly reduced and concentrated in the satisfactory range (±5 mph) (Figure 3.19) Overall, the results show evidence that queue warning messages help smooth traffic by reducing the speed difference across detector stations.

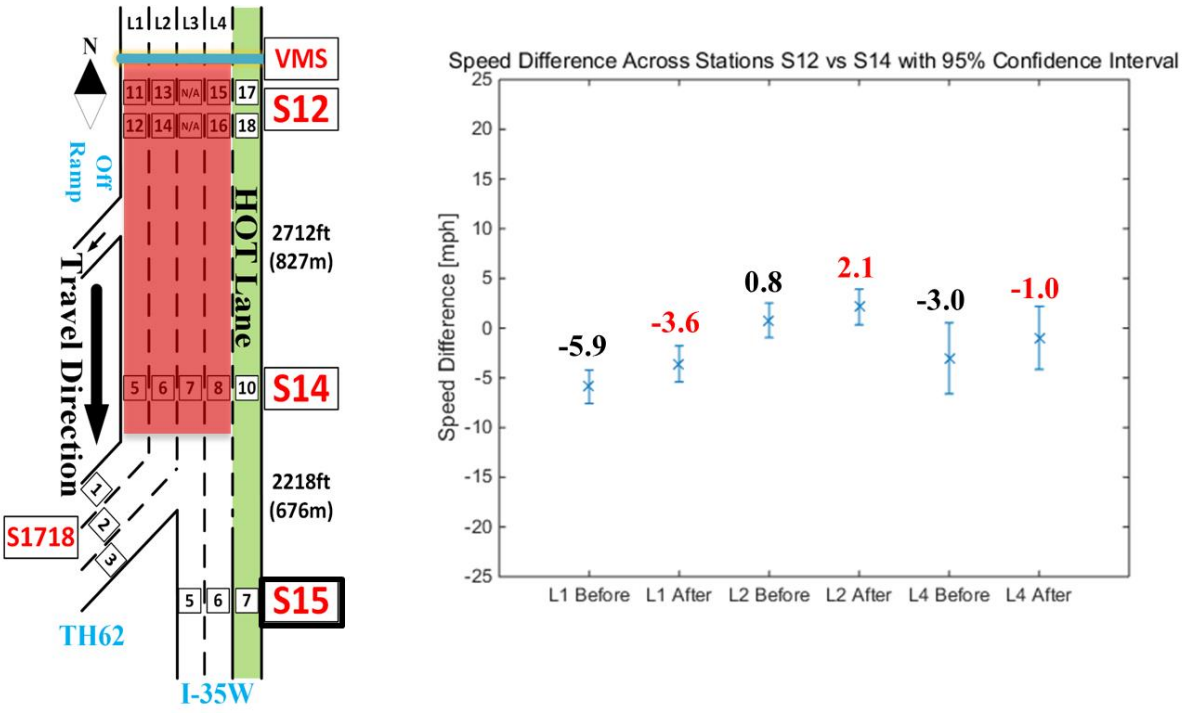

Figure 3.18 Speed difference across Stations S12 and S14

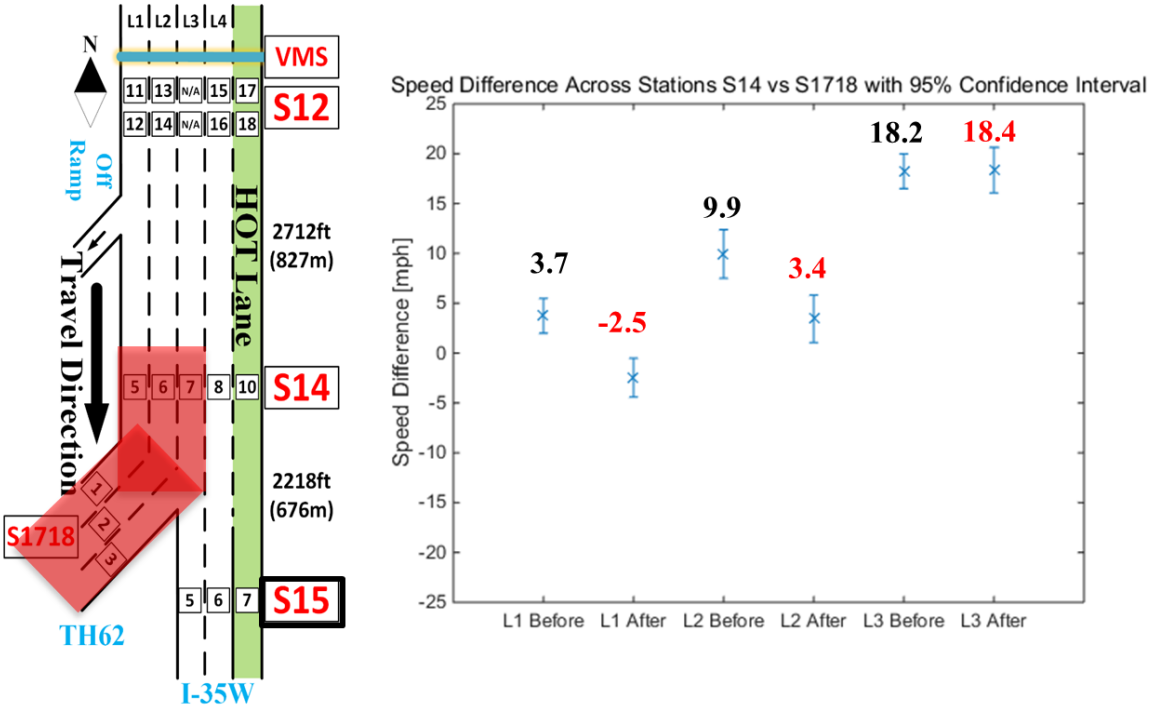

Figure 3.19 Speed difference across Stations S14 and S1718

3.6.1.8 Speed Changes in Morning Peak and Evening Peak

Based on field observations, I-35W tends to be congested during morning peak period whereas TH62 tends to be congested during evening peak period. These two cases were selected for further study. From the data collected, 59.4% of the warning messages triggered from I-35W were in the morning peak, and 57.8% of the warning messages triggered from TH62 were in the evening peak. Comparing before and after cases, no significant change of speed at S12 was found. At S14, after deployment, the standard deviation of speed on Lane 4 during the morning peak decreased (Figure 3.20), the mean value and standard deviation of speed on Lane 3 (message triggered from TH62 direction) during the evening peak increased, and the standard deviation of speed on Lane 1 during the evening peak decreased (Figure 3.21). The results were similar to those derived from the all-day data in Section 3.6.1.4 and Section 3.6.1.5.

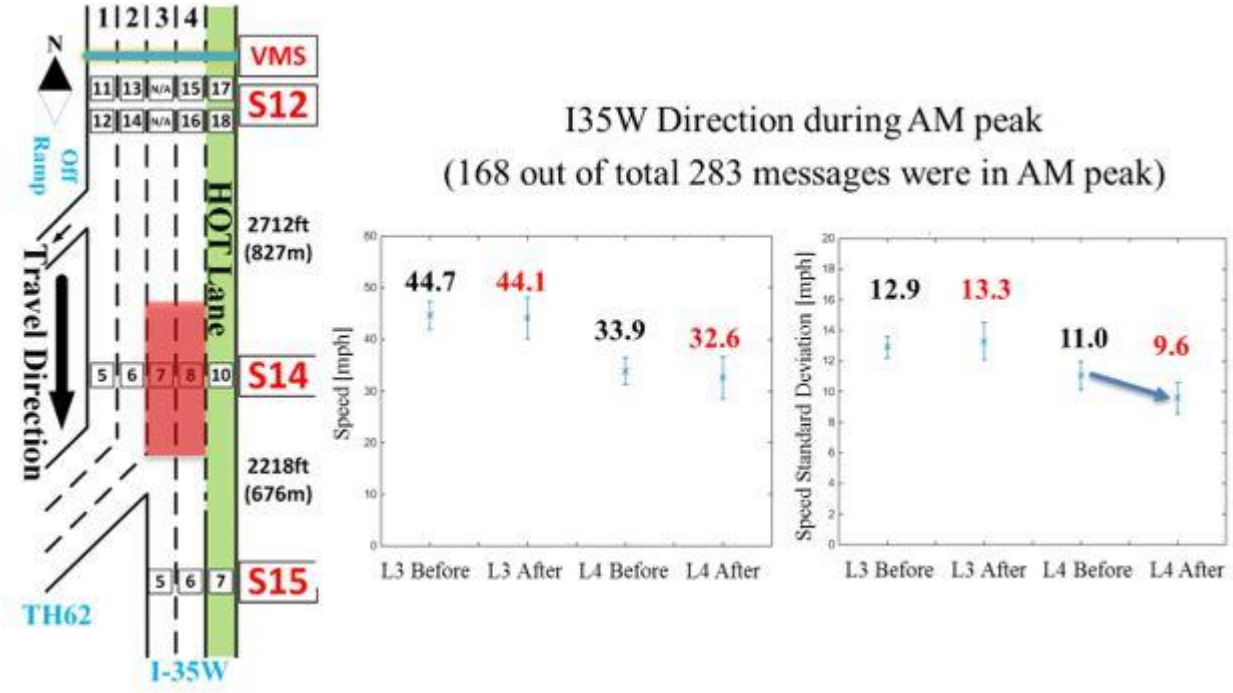

Figure 3.20 Mean value and standard deviation of speed in morning peak in I-35W direction

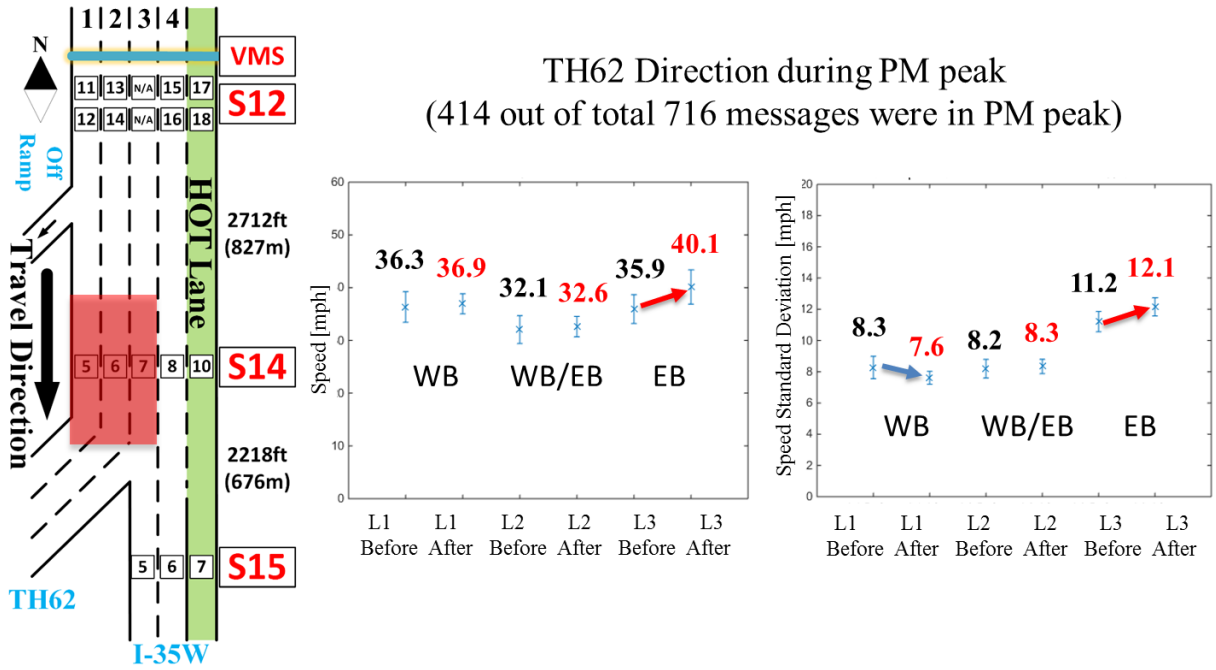

Figure 3.21 Mean value and standard deviation of speed in evening peak in TH62 direction

3.6.1.9 Summary of Evaluation Results

With the evaluation results above, we come to the following preliminary conclusions.

1. In general, travelers on I-35W responded to the queue warning message "SLOW TRAFFIC AHEAD" and the traffic conditions with and without messages showed statistical differences.
2. The queue warning system was able to smooth the traffic by reducing the speed variance at the downstream locations and speed difference between the upstream and downstream locations thereby reducing the risk of rear-end crashes and potentially improving mobility.
3. It took drivers some time from seeing the messages to taking actions such as slowing down their vehicles. As a consequence, queue warning messages had little effect on the traffic conditions near the VMS (S12 in this case) but had an clear impact on the traffic at the downstream locations (S14 in this case).
4. The standard deviation of speed at the fork in the road was increased when the traffic condition at the location further downstream on TH62 was continually congested. This may be due to the fact that the traffic state in this case was influenced more by the downstream congestion rather than the upstream arrivals which kept the queue warning message from being effective.

There was no significant difference between the warning message's effects on the morning peak and the evening peak.

3.7 DISCUSSION

Rear-end crashes are the most frequent type of crashes observed on freeways and research has shown that freeway rear-end crashes tend to occur in extended congested traffic situations where the speed variation is large, e.g. end-of-queue locations. One of the prevailing active traffic management strategies is the ILCS system that displays messages to warn drivers about upcoming queues and caution them to adjust their speed to avoid potential rear-end collisions. One main component of such active traffic management strategies is the real-time queue estimation algorithm which depends highly on the data being utilized.

In this project, a real-time queue warning system was developed and deployed on a freeway segment on I-35W south of Minneapolis, MN. Benefiting from a previously-developed data collection system , five sets of data collection devices were installed on the segment of interest. High-resolution detector actuation data were then collected from the field. By taking advantage of such high-resolution event-based data, every traffic state change at detector locations can be identified within a few seconds. Shockwave analysis is adopted to develop the real-time queue estimation algorithm. The algorithm runs locally in any freeway segment between an upstream detector and a downstream detector, estimating the length and duration of a queue once the queue is detected by the downstream detector. When the queue extends upstream of the upstream detector, the algorithm stops estimating it with further estimation of the queue being provided by the same algorithm running in the next segment upstream. Due to the differences in traffic states between lanes (e.g., lanes to different directions of a diverge junction), one instance of the algorithm runs for each lane. The impact of lane changes is considered as well by analyzing traffic data from detectors on adjacent lanes. The algorithm also has limited capability of prediction as to the time when a queue will be formed or cleared at any position in this segment nor can it predict the queue length in this segment at any time in the near future. The proposed algorithm was tested with field data and validated by video captured in the field.

The queue warning system was tested in the field for three weeks, showing the queue warning message “SLOW TRAFFIC AHEAD” to travelers when a queue was estimated at downstream locations. Before that, the system had also been running for three weeks without actually showing messages. The high-resolution data from loop detectors, the queue warning system log files archiving the start time, duration, and location of triggered messages (including those not shown on VMS before field test), and videos from MnDOT cameras were used to evaluate the queue warning system. By comparing the before and after cases, the impacts of warning messages were studied. Promisingly, for most of the studied locations, the study showed that queue warning messages helped to reduce the speed variance near the queue locations and the speed difference between upstream and downstream locations. This also implies a satisfactory level of compliance rate by drivers.

CHAPTER 4: CONCLUDING REMARKS

The research described in this report is aimed at developing and field-testing two queue warning systems following different philosophies in regard to rear-end collision safety. The MQWA system philosophy follows the premise that freeway rear-end collisions tend to occur in extended stop-and-go traffic or at end-of-queue locations. The MQWA system prototype was deployed and evaluated in Minneapolis, MN, on I-35W southbound where conditions supported this hypothesis. QWARN is based on the hypothesis that not all congestion events are dangerous and that certain traffic conditions that are crash prone regardless of whether they result in standing queues or not. Such CPCs can be isolated, fast moving shockwaves, involving only a small number of vehicles in the deceleration-stop-acceleration cycle. One location where such conditions have been identified and result in more than 100 crashes per year is the westbound section of I-94 in downtown Minneapolis, MN. This location was selected for the QWARN deployment and evaluation.

Although, each system was evaluated using different methodologies, both have demonstrated a positive effect on driver behavior. The MQWA system on I-35W has smoothed the traffic flow by reducing the speed variance at downstream locations and speed difference between upstream and downstream. The evaluation period (three weeks) was short so no data on the actual influence of the system on crash rates were collected. QWARN's deployment on I-94 has resulted in a 22% reduction in crashes and a 54% reduction in near-crash events during a three-month evaluation period. In both cases, the short evaluation periods can only show promise and longer traffic safety studies are needed to show whether the systems will have a lasting effect on safety in their respective corridors. Following the reporting of the evaluation results, MnDOT has lifted the restriction that the system only operate between noon and 8 p.m. and now allows the alarms to be displayed any time the system detects a crash-prone condition.

At the time this report was written, both systems were in operation. Although, there are no current plans to expand the deployment of the MQWA system, MnDOT expressed the desire to deploy QWARN in two upstream locations on the I-94 WB corridor in anticipation of CPCs following the beginning of construction on the stretch of I-94 QWARN is currently deployed on. Although funding has not been secured yet for such an expansion, the Minnesota Traffic Observatory is continuing to refine QWARN as well as the collect video and detector data to facilitate a longer-term evaluation.

REFERENCES

1. Early Estimate of Motor Vehicle Traffic Fatalities in 2014, https://crashstats.nhtsa.dot.gov/Api/Public/ViewPublication/812160

2. Benefit-Cost Analysis for Transportation Projects, http://www.dot.state.mn.us/planning/program/appendix_a.html

3. Minnesota Traffic Crashes in 2014, https://dps.mn.gov/divisions/ots/reports-statistics/Documents/2014-crash-facts.pdf https://dps.mn.gov/divisions/ots/reports-statistics/Documents/2014-crash-facts.pdf

4. Hourdos, J., Garg, V., Michalopoulos, P., & Davis, G. (2006). Real-Time Detection of Crash-Prone Conditions at Freeway High-Crash Locations. *Transportation Research Record*, 1968(1), 83–91. doi: 10.3141/1968-10

5. Qiu, L., & Nixon, W. A. (2008). Effects of Adverse Weather on Traffic Crashes: Systematic Review and Meta-Analysis. *Transportation Research Record*, 2055, 139–146. doi:10.3141/2055-16

6. Kopelias, P., Papadimitriou, F., Papandreou, K., & Prevedouros, P. (2007). Urban Freeway Crash Analysis: Geometric, Operational, and Weather Effects on Crash Number and Severity. *Transportation Research Record*, 2015, 123–131. doi:10.3141/2015-14

7. Golob, T. F., & Recker, W. W. (2003). Relationships Among Urban Freeway Accidents, Traffic Flow, Weather, and Lighting Conditions. *Journal of Transportation Engineering*, 129(August), 342–353. doi:10.1061/(ASCE)0733-947X (2003)129:4(342)

8. Zheng, Z., Ahn, S., & Monsere, C. M. (2010). Impact of traffic oscillations on freeway crash occurrences. *Accident Analysis and Prevention*, 42(2), 626–636. doi: 10.1016/j.aap.2009.10.009

9. Abdel-Aty, M., Uddin, N., Pande, A., Abdalla, F., & Hsia, L. (2004). Predicting Freeway Crashes from Loop Detector Data by Matched Case-Control Logistic Regression. *Transportation Research Record*.

10. Caliendo, C., Guida, M., & Parisi, A. (2007). A crash-prediction model for multilane roads. *Accident Analysis and Prevention*, 39(4), 657–670. doi: 10.1016/ j.aap. 2006.10.012

11. Pei, X., Wong, S. C., & Sze, N. N. (2011). A joint-probability approach to crash prediction models. *Accident Analysis and Prevention*, 43(3), 1160–1166. doi: 10.1016/ j.aap. 2010.12.026

12. Naderan, A., & Shahi, J. (2010). Aggregate crash prediction models: Introducing crash generation concept. *Accident Analysis and Prevention*, 42(1), 339–346. doi: 10.1016/ j.aap. 2009.08.020

13. Montella, A., Colantuoni, L., & Lamberti, R. (2008). Crash Prediction Models for Rural Motorways. *Transportation Research Record*, 2083, 180–189. doi:10.3141/2083-21

14. Abdel-Aty, M. A., & Pemmanaboina, R. (2006). Calibrating a real-time traffic crash-prediction model using archived weather and ITS traffic data. *IEEE Transactions on Intelligent Transportation Systems*, 7(2), 167–174.

15. Abdel-Aty, M., & Gayah, V. (2010). Real-Time Crash Risk Reduction on Freeways Using Coordinated and Uncoordinated Ramp Metering Approaches. *Journal of Transportation Engineering*.

16. Lee, C., Hellinga, B., & Saccomanno, F. (2003). Real-Time Crash Prediction Model for Application to Crash Prevention in Freeway Traffic. *Transportation Research Record*, 1840, 67–77. doi:10.3141/1840-08

17. Khan, A. Intelligent infrastructure-based queue-end warning system for avoiding rear impacts. *IET Intelligent Transportation Systems*, Vol. 1, No. 2, 2007, p. 138.

18. ARTBA Work Zone Safety Consortium. Innovative End-of Queue Warning System Reduces Crashes Up to 45%. ARTBA Work Zone Safety Consortium, 2015.

19. Pesti, G., P. Wiles, R. Cheu, P. Songchitruska, J. Shelton, and S. Cooner. (2007) Traffic Control Strategies for Congested Freeways and Work Zones. Texas Department of Transportation.

20. Delta Highway Queue Warning System Evaluation - Final Technical Memorandum. http://www.kittelson.com/projects/intelligent-transportation-systems-its-statewide-evaluations. Accessed Jul. 19, 2016.

21. Mahmassani, H., Rakha, H., Hubbard, E., and Lukasik, D. Concept Development and Needs Identification for Intelligent Network Flow Optimization (INFLO). USDOT ITS Joint Program Office, 2012.

22. Hourdakis, J., Michalopoulos, P. G., and Morris, T. (2004) Deployment of Wireless Mobile Detection and Surveillance for Data-Intensive Applications. In Transportation Research Record, pp. 140–148.

23. Jones, T., and Potts R. "The Measurement of Acceleration Noise-A Traffic Parameter." *Operations Research* 10.6 (1962): 745-63. Web.

24. Helly, W., and Baker, P.G., (1965). “Acceleration noise in a congested signalized environment.” Vehicular Traffic Science. Proceedings of the Third International Symposium on the Theory of Traffic Flow. pp. 55-61.

25. Greenshields, B. D. (1961) “Quality of Traffic Flow, Quality and Theory of Traffic Flow.” Symposium, Bureau of Highway Traffic, Yale University, New Haven, Conn. pp.3-40.

26. Phillips, W. F., (1979). “A kinetic model for traffic flow with continuum implications”. *Transportation Planning and Technology* 5, 131-138.

27. Drew, D., (1968) *Traffic Flow Control and Theor*y, McGraw Hill.

28. Hourdos, J. (2005) Crash prone traffic flow dynamics: Identification and real-time detection. Ph.D. dissertation, University of Minnesota, 315 pages.

29. Pande, A. and Abdel-Aty, M. (2006) Assessment of freeway traffic parameters leading to lane-change related collisions, *Accident Analysis & Prevention*, 38, (5), p. 936-948

30. Akcelik, R. (1998), A queue model for HCM 2000, ARRB Transportation Research Ltd., Vermont South, Australia.

31. Balke, K., Charara, H. and Parker, R. (2005), Development of a traffic signal performance measurement system (TSPMS), Texas Transportation Institute, The Texas A&M University System College Station, TX.

32. Bertini, R.L., Boice, S. and Bogenberger, K. (2006), Dynamics of Variable Speed Limit System Surrounding Bottleneck on German Autobahn, *Transportation Research Record*, no. 1978, pp. 149-159.

33. Catling, I. (1977), A time dependent approach to junction delays, *Traffic Engineering and Control*, 18, (11), pp. 520-526.

34. Chan, C. (2012), Monitoring and Improving Roadway Surface Conditions For Safe Driving Environment and Sustainable Infrastructure, University of California Berkeley – PATH, Richmond Field Station, Bldg., Richmond, CA.

35. Chang, T. and Lin, J. 2000, "Optimal signal timing for an oversaturated intersection", *Transportation Research Part B: Methodological*, 34, (6), 471-491.

36. Chatterjee, K., Hounsell, N.B., Firmin, P.E. and Bonsall, P.W. (2002), Driver response to variable message sign information in London, *Transportation Research Part C: Emerging Technologies*, 10, (2), 149-169.

37. Cheng, Y., Qin, X., Jin, J. and Ran, B. (2012), An Exploratory Shockwave Approach to Estimating Queue Length Using Probe Trajectories, *Journal of intelligent transportation systems*, 16, (1), 12-23.

38. Comert, G. and Cetin, M. (2009), Queue length estimation from probe vehicle location and the impacts of sample size, *European Journal of Operational Research*, 197, (1), 196-202.

39. Cronje, W.B. (1983a), Analysis of existing formulas for delay, overflow, and stops, *Transportation Research Record*, 905, 89-93.

40. Cronje, W.B. (1983b), Derivation of equations for queue length, stops, and delay for fixed-cycle traffic signals, *Transportation Research Record*, 905, 93-95.

41. Elefteriadou, L., R. P. Roess and W. R. McShane, (1995). Probabilistic Nature of Breakdown at Freeway Merge Junctions. *Transportation Research Record*, 1484, 80-89.

42. Gazis, D.C. (1964), Optimum Control of a System of Oversaturated Intersections, *Operations Research*, 12 (6), 815-831.

43. Gazis, D.C. 1974, Traffic Science, New York, N.Y. Wiley-Interscience, Inc.

44. Ghosh-Dastidar, S. and Adeli, H. (2006), Neural Network-Wavelet Microsimulation Model for Delay and Queue Length Estimation at Freeway Work Zones, *Journal of Transportation Engineering*, 132 (4), 331-341.

45. Green, D.H. (1967), Control of Oversaturated Intersections, *Operations research*, 18 (2), 161-173.

46. Gregory, C. (2004), Managing Traffic During Poor Visibility "A Journey Through the Fog". National Highway Visibility Conference (NHVC 2004), Madison, Wisconsin.

47. Harder, K. and Bloomfield, J. (August 2012), Investigating the Effectiveness of Intelligent Lane Control Signals on Driver Behavior, Minneapolis, MN, Center for Design in Health, College of Design, University of Minnesota.

48. Hassan, H.M., Abdel-Aty, M., Choi, K. and Algadhi, S.A. (2012), "Driver Behavior and Preferences for Changeable Message Signs and Variable Speed Limits in Reduced Visibility Conditions", *Journal of Intelligent Transportation Systems*, 16 (3), 132-146.

49. Hiribarren, G. and Herrera, J.C. (2014), Real time traffic states estimation on arterials based on trajectory data, *Transportation Research Part B: Methodological*, 69 (0), 19-30.

50. Hourdos, J., Garg, V. and Michalopoulos, P.G. (September 2008a), Accident Prevention Based on Automatic Detection of Accident Prone Traffic Conditions: Phase I, Minneapolis, MN: Intelligent Transportation Systems Institute, Center for Transportation Studies, University of Minnesota.

51. Hourdos, J., Xin, W. and Michalopoulos, P.G. (December 2008b), Development of Real-Time Traffic Adaptive Crash Reduction Measures for the Westbound I-94/35W Commons Section, Minneapolis, MN: Intelligent Transportation Systems Institute, Center for Transportation Studies, University of Minnesota.

52. Jiang, Y. (2001), A model for estimating traffic delays and vehicle queues at freeway work zones, *Journal of the Transportation Research Forum*, 40 (4), 65-81.

53. Karim, A. and Adeli, H. (2003), "Radial Basis Function Neural Network for Work Zone Capacity and Queue Estimation", *Journal of Transportation Engineering*, 129 (5), 494-503.

54. Khan, A.M. (2007), Intelligent infrastructure-based queue-end warning system for avoiding rear impacts, *Intelligent Transport Systems*, IET, 1 (2), 138-143.

55. Lee, C. and Abdel-Aty, M. (2008), Testing Effects of Warning Messages and Variable Speed Limits on Driver Behavior Using Driving Simulator, *Transportation Research Record*, 2069 (-1), 55-64.

56. Lighthill, M.J. and Whitham, G.B. (1955), On Kinematic Waves. II. A Theory of Traffic Flow on Long Crowded Roads, *Proceedings of the Royal Society of London A: Mathematical, Physical and Engineering Sciences*, 229 (1178), 317-345.

57. Liu, H.X. and Ma, W. (2009), A virtual vehicle probe model for time-dependent travel time estimation on signalized arterials, *Transportation Research Part C: Emerging Technologies*, 17 (1), 11-26.

58. Liu, H.X., Wu, X., Ma, W. and Hu, H. (2009), Real-time queue length estimation for congested signalized intersections, *Transportation Research Part C: Emerging Technologies*, 17 (4), 412-427.

59. MacCarley, C.A. (2005a), Methods and Metrics for Evaluation of an Automated Real-Time Driver Warning System, *Transportation Research Record*, 1937, 87-95.

60. MacCarley, C.A. (2005b), Evaluation of Traffic Safety Influence Based on Historical Collision data.

61. Maerivoet, S. and De Moor, B. 2005, "Traffic Flow Theory".

62. Michalopoulos, P.G. and Stephanopoulos, G. (1977a), Oversaturated signal systems with queue length constraints—I: Single intersection, *Transportation Research*, 11 (6), 413-421.

63. Michalopoulos, P.G. and Stephanopoulos, G. (1977b), Oversaturated signal systems with queue length constraints—II: Systems of intersections, *Transportation Research*, 11 (6), 423-428.

64. Michalopoulos, P. and Stephanopoulos, G. (1981), An application of shock wave theory to traffic signal control, *Transportation Research Part B: Methodological*, 15 (1), 35-51.

65. Mirchandani, P.B. and Zou, N. (2007), Queuing Models for Analysis of Traffic Adaptive Signal Control, *Intelligent Transportation Systems, IEEE Transactions*, 8 (1), 50-59.

66. Newell, G.F. (1965), Approximation Methods for Queues with Application to the Fixed-Cycle traffic Light, *SIAM Review*, 7 (2), 223-240.

67. Richards, P.I. (1956), Shock Waves on the Highway, *Operations Research*, 4 (1), 42-51.

68. Robertson, D.I. (1969), TRANSY: A traffic network study tool, Road Research Laboratory, Crowthorne.

69. Rouphail, N.M., Courage, K.G. and Strong, D.W. (2006), New Calculation Method for Existing and Extended Highway Capacity Manual Delay Estimation Procedures, Transportation Research Board 85th Annual Meeting, Washington, DC.

70. Sharma, A., Bullock, D.M. and Bonneson, J.A. (2007), Input–Output and Hybrid Techniques for Real-Time Prediction of Delay and Maximum Queue Length at Signalized Intersections, *Transportation Research Record*, 2035, 69-80.

71. Sheu, J., Chou, Y. and Shen, L. (2001), A stochastic estimation approach to real-time prediction of incident effects on freeway traffic congestion, *Transportation Research Part B: Methodological,* 35 (6), 575-592.

72. Skabardonis, A. and Geroliminis, N. (2008), "Real-time Monitoring and Control on Signalized Arterials", *Journal of Intelligent Transportation Systems*, 12 (2), 64-74.

73. Transportation Research Board 2010, Highway Capacity Manual 2000.

74. Vigos, G., Papageorgiou, M. and Wang, Y. (2008), Real-time estimation of vehicle-count within signalized links, *Transportation Research Part C: Emerging Technologies*, 16 (1), 18-35.

75. Webster, F.V. (1958), Traffic Signal Settings, *Road Research Technical Paper*, vol. 39.

76. Webster, F.V. and Cobbe, B.M. 1966, Traffic signals, H.M.S.O., London.

77. Weng, J. and Meng, Q. (2013), Estimating capacity and traffic delay in work zones: An overview, *Transportation Research Part C: Emerging Technologies*, 35, 34-45.

78. Wrapson, W., Harré, N. and Murrell, P. (2006), Reductions in driver speed using posted feedback of speeding information: Social comparison or implied surveillance?, *Accident Analysis & Prevention*, 38 (6), 1119-1126.

79. Wu, J., Jin, X. and Horowitz, A. (2008), Methodologies for Estimating Vehicle Queue Length at Metered On-Ramps, *Transportation Research Record*, 2047, (-1), 75-82.

80. Wu, X. and Liu, H.X. (2011), A shockwave profile model for traffic flow on congested urban arterials, *Transportation Research Part B: Methodological*, 45 (10), 1768-1786.

81. Minnesota Dept. of Transportation (2002), Freeway Volume-Crash Summary, Twin Cities Metropolitan area. Systems and Research Section, Office of Traffic Engineering, Minnesota Dept. of Transportation. St. Paul.